Chronic exposure to odors at naturally occurring concentrations triggers limited plasticity in early stages of *Drosophila* olfactory processing

Zhannetta V. Gugel, Elizabeth Maurais, and Elizabeth J. Hong*

Division of Biology and Biological Engineering, California Institute of Technology, Pasadena, CA

*Correspondence to ejhong@caltech.edu

ABSTRACT

In insects and mammals, olfactory experience in early life alters olfactory behavior and function in later life. In the vinegar fly *Drosophila*, flies chronically exposed to a high concentration of a monomolecular odor exhibit reduced behavioral aversion to the familiar odor when it is re-encountered. This change in olfactory behavior has been attributed to selective decreases in the sensitivity of second-order olfactory projection neurons (PNs) in the antennal lobe that respond to the overrepresented odor. However, since odorant compounds do not occur at similarly high concentrations in natural sources, the role of odor experience-dependent plasticity in natural environments is unclear. Here, we investigated olfactory plasticity in the antennal lobe of flies chronically exposed to odors at concentrations that are typically encountered in natural odor sources. These stimuli were chosen to each strongly and selectively excite a single PN type to saturating firing rates, facilitating a rigorous assessment of the selectivity of olfactory plasticity for PNs directly excited by overrepresented stimuli. Unexpectedly, we found that chronic exposure to three such odors did not result in decreased PN sensitivity, but rather mildly increased responses to weak stimuli in most PN types. Odor-evoked PN activity in response to stronger stimuli was mostly unaffected by odor experience. When present, plasticity was observed broadly in multiple PN types and thus was not selective for PNs receiving direct input

from the chronically active ORNs. We further investigated the DL5 olfactory coding channel and found that chronic odor-mediated excitation of its input ORNs did not affect PN intrinsic properties, local inhibitory innervation, ORN responses, or ORN-PN synaptic strength; however, broad-acting lateral excitation evoked by some odors was increased. These results show that PN odor coding is only mildly affected by strong persistent activation of a single olfactory input, highlighting the stability of early stages of insect olfactory processing to significant perturbations in the sensory environment.

INTRODUCTION

In many animals, early sensory experience modifies the structure and function of sensory systems. For example, visual experience is required for the normal development of the mammalian visual system[1]. One prominent hypothesis is that an important function of sensory plasticity is to adapt circuit function to the current statistical distribution of sensory inputs in the environment, allowing for more efficient sensory codes[2–5]. This hypothesis requires sensory driven plasticity to be stimulus- and cell-specific; in other words, neurons encoding specific stimuli that occur very frequently (or very rarely) in the environment should be selectively affected by plasticity[6–11]. The circuit mechanisms that would implement such use-dependent, input-specific plasticity are not well understood.

The orderly structure of the olfactory system provides a useful experimental model for investigating the synaptic and circuit mechanisms mediating stimulus-selective sensory plasticity. In insect and vertebrate olfactory circuits, sensory information is organized in anatomically discrete synaptic compartments, called glomeruli. Each glomerulus receives direct input from only a single class of primary olfactory receptor neurons (ORNs), all expressing the same olfactory receptor, and, thus, all sensitive to the same chemical feature(s)[12–15]. Furthermore,

the dendrites of each second-order uniglomerular projection neuron (PN) arborize in only a single glomerulus, so each PN receives direct input from only a single class of ORNs[16]. In the vinegar fly *Drosophila melanogaster*, the majority of odorant receptors and ORN subtypes have been mapped to their corresponding glomeruli in the brain[17–19], and the odor tuning profiles for a large subset of the odorant receptors have been characterized[19–23]. As a result, specific odors can be used to selectively target neural activation of defined olfactory channels[24,25]. Together with the highly compartmentalized organization of the circuit, these features make the fly olfactory system a powerful experimental model for studying the specificity of sensory plasticity.

Passive odor experience in early life, in the absence of explicit coupling to reward or punishment, can alter olfactory circuit structure and function, including olfactory preference or discrimination ability[26,27]. For instance, chronic odor exposure in rodents can trigger changes in the structural connectivity and physiological response properties of neurons in the olfactory bulb, the first central processing area for odors in the brain[10,28–31]. In insects, passive odor experience has also been found to impact olfactory processing in the antennal lobe, the insect analog of the olfactory bulb[32–34]. Chronic exposure to high concentrations of monomolecular odor, stimuli which are typically strongly aversive, reduces behavioral avoidance towards the familiar odor selectively when it is reencountered[6,35,36]; in parallel, structural alterations in glomerular volume are also observed[6,8,35–38]. Odor experience-dependent reductions in olfactory aversion have been interpreted as a form of long-term behavioral habituation to overrepresented stimuli in the environment and are attributed to reduced PN responses in flies chronically exposed to odor[6,8] (see also[38]). Importantly, since behavioral plasticity is odor-specific and does not generalize to other odors, structural and functional neural plasticity are also believed to be glomerulus-specific (and thus odor-specific), acting to selectively reduce the olfactory sensitivity of only those PNs activated by the overrepresented stimuli. However, since past studies exposed animals to

intense monomolecular odors[6,8,35–37,39] (e.g., 10% isoamyl acetate or 20% ethyl butyrate), which typically excite many classes of ORN inputs, stringent testing of this idea has not been possible.

Arriving at a systematic understanding of how odor experience modifies the structure and function of olfactory circuits has been challenging for several reasons. First, diverse protocols are used for odor exposure, which vary in the degree of control over odor delivery, odor concentration, timing, as well as context (availability of food, mates, etc). Second, different studies focus on different odors and glomeruli, and the high dimensionality of chemical stimulus space and olfactory circuits presents unique challenges to methodical exploration. Finally, nearly all studies, in insects or in mammals, use very high concentrations of monomolecular odorants during the exposure period, at intensities that are not encountered in the natural word (see Discussion). Odors at these concentrations broadly activate many classes of ORNs, complicating the evaluation of the contributions of direct and indirect activity for triggering plasticity in each olfactory processing channel. Some of the major outstanding questions include: 1) How does olfactory plasticity modify circuit function in the context of odor environments that could be realistically encountered in the natural world? 2) To what extent is plasticity selective for the olfactory channel(s) which directly detect overrepresented odors? 3) Are the rules governing olfactory plasticity the same or different across glomeruli?

The goals of this study were to investigate the impact of olfactory experience on odor coding in the *Drosophila* antennal lobe, using a physiologically plausible olfactory environment that strongly but selectively increases neural activity in a single class of ORNs. This experimental design allowed us to readily distinguish the effects of direct versus indirect chronic activity on specific classes of PNs, which convey neural output from the antennal lobe to higher olfactory centers in the fly brain. This distinction is important because it allowed us to unambiguously evaluate whether olfactory plasticity selectively affects only the chronically active glomerulus. Investigating three different glomerular channels, we unexpectedly observed that, rather than

reduce PN sensitivity, chronic odor exposure resulted in mild increases in PN sensitivity, particularly in response to weak odors. PN responses to moderate or strong stimuli were mostly unaffected. Changes in odor responses, when present, were observed broadly, both in glomeruli that receive either direct or indirect activity from the chronically active ORN class. These results diverge from current models suggesting that odor-specific behavioral plasticity arises from glomerulus-specific long-term adaptation of PN responses in the antennal lobe[6,8,39,40] and motivate the search for other circuit mechanisms mediating how olfactory experience alters behavior towards familiar odors.

RESULTS

Chronic activation of direct ORN input modestly increases PN responses to weak stimuli

To investigate how odors that are overrepresented in the environment are encoded by the fly olfactory system, we chronically exposed flies to 1 sec pulses of a specific monomolecular odorant, introduced into the bottle in which they normally grow (Figure 1A). We chose to use the odors at concentrations previously shown to selectively activate a single class of ORNs[24,41], in order to simplify the investigation of odor coding in postsynaptic PNs receiving direct versus indirect chronic excitation. An additional criterion was that the odor stimuli drive strong, consistent, and saturating levels of firing in PNs receiving direct input from the activated ORN class (in other words, using a higher concentration of odor would not reliably drive higher firing rates in the PN type that is directly excited by that stimulus). Photoionization measurements of the odor concentration in the rearing bottle demonstrated that the stimulus amplitude changed <20% over 12 hours (Figure 1B), after which the odor source was refreshed. The largest decrease in delivered odor concentration occurred within the first two hours and slowed significantly thereafter. Odors were pulsed to minimize neural adaptation to the odor, and the interval

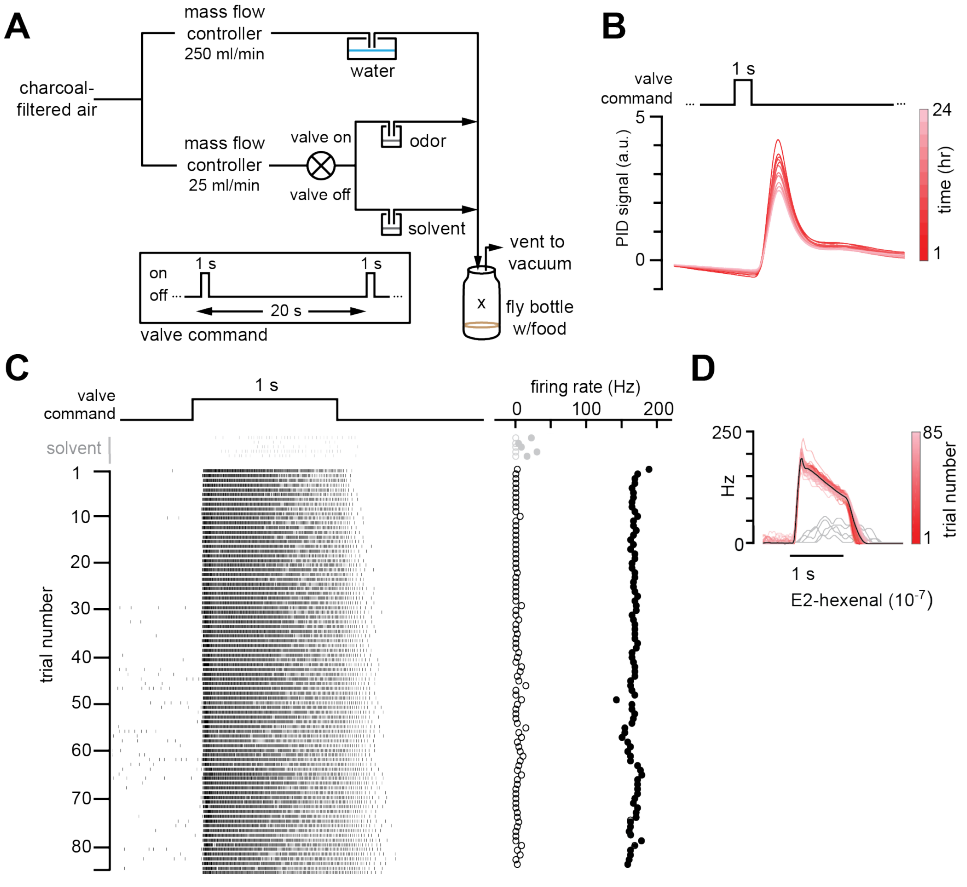

Figure 1: Chronic stimulation of olfactory neurons in a controlled odor environment.
A) Schematic of experimental setup for chronic odor exposure. The valve was opened for 1 s every 20 s to deliver odor. See **Methods** (*Chronic Odor Exposure*) for details.
B) Photoionization detector measurement of odor concentration at the center of the fly bottle ("X" in **A**) during chronic odor exposure to 2-butanone (10^{-4}) over the course of 24 hours. Each trace is the odor profile averaged across 45 consecutive odor pulses (collected over 15 min), sampled every two hours over a 24-hour period.
C) Raster plots of the spiking responses in an example DL5 PN to a 1 s pulse of either solvent (paraffin oil, grey) or E2-hexenal (10^{-7}, black) in consecutive trials spaced 20 seconds apart. Recordings were established from a fly immediately after two days of chronic exposure to E2-hexenal (10^{-7}) as in **A**). Spontaneous (open circles) and stimulus-evoked (filled circles) firing rates are plotted for each trial.
D) Peristimulus time histograms of measurements in **C**) show that the odor environment reliably evokes high levels of PN firing across presentation trials. The average odor-evoked response across all trials is in black. Responses to presentation of solvent are overlaid in grey.

between odor pulses delivered to the bottle was 20 seconds. Pilot recordings showed that, at this interstimulus interval, the odors reliably activated cognate PNs to saturating or near saturating firing rates over many trials (Figure 1C-D, and data not shown; see also Figure 2Q). PN response duration to the 1 s stimulus increased systematically and substantially across successive odor presentations. Thus, although the odor stimuli to which we exposed flies were of significantly lower concentration than what has been previously used to investigate the effect

of chronic odor exposure on PNs[6,8,38], these stimuli drove high, reliable, near saturating levels of firing in their corresponding PN type (Figure 1C, data not shown). On average, this odor exposure protocol more than doubled the average firing rate of the targeted PN and elicited more than a million extra spikes in the activated PN over the course of the two-day period of exposure (see Methods).

Using these conditions, newly eclosed flies were chronically exposed for two days to E2-hexenal (10^{-7}), which selectively activates ORNs projecting to glomerulus DL5, or to solvent (as a control) (see Methods). On day three, we established fluorescently guided, whole-cell current clamp recordings from uniglomerular PNs receiving direct input from the DL5 glomerulus (hereafter referred to as DL5 PNs, Figure 2A), and measured their responses to a concentration series of E2-hexenal. DL5 PNs were identified and targeted for recording based on their expression of GFP, mediated by a genetic driver that specifically labels this cell type (see Methods). DL5 PN responses elicited by moderate to high concentrations of E2-hexenal ($>10^{-8}$) were unchanged in E2-hexenal exposed flies, as compared to controls (Figure 2B, 2Q). However, low concentrations of E2-hexenal (10^{-10} to 10^{-9}) elicited increased levels of odor-evoked membrane depolarization in DL5 PNs from E2-hexenal exposed flies compared to solvent-exposed flies (Figure 2B). The heightened depolarization of DL5 PNs by weak stimuli corresponded to higher average rates of odor-evoked spiking (Figure 2D).

We quantified these effects by calculating the total depolarization and average evoked firing rate during the first 500 ms after nominal stimulus onset (Figure 2C, 2E). To determine if any differences were arising by chance, we used permutation testing in which we iteratively shuffled the experimental labels of each measurement (E2-hexenal versus solvent exposure) within each stimulus. P-values were calculated directly from the fraction of 10,000 shuffled trials in which the absolute difference between the simulated group means was larger than or equal to the actual observed absolute mean difference (see Methods). This statistical analysis

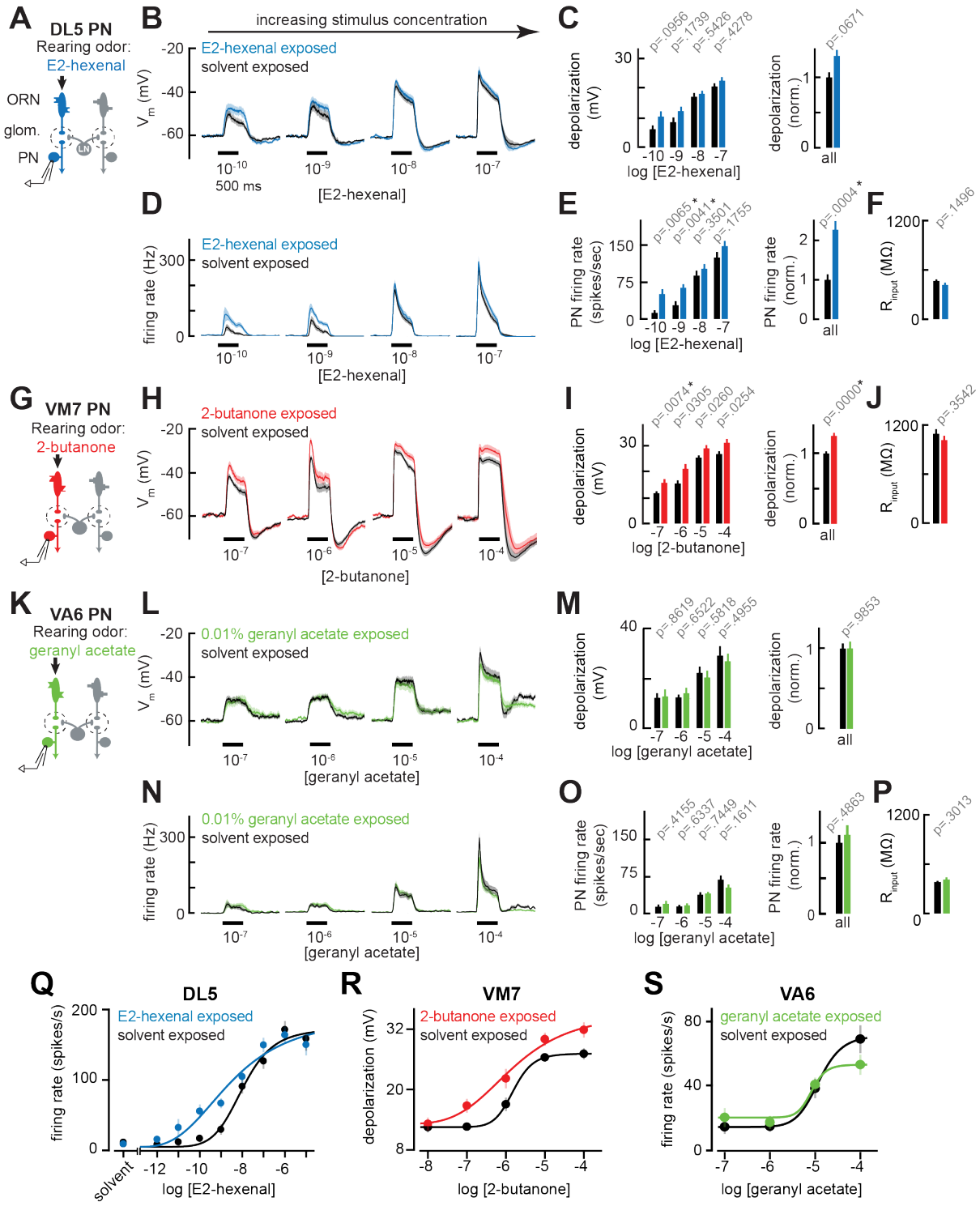

Figure 2: Chronic excitation of direct presynaptic ORN input can modestly enhance PN sensitivity to weak stimuli.

A) Schematic of experimental setup for **B-F**). Recordings were established from DL5 PNs that receive direct presynaptic input from the ORN class (ab4a) chronically activated by the rearing odor (E2-hexenal, 10^{-7}), *n*=7-19 cells.

Figure 2 *(continued)*: B) Odor-evoked depolarization in DL5 PNs in response to varying concentrations of E2-hexenal from flies chronically exposed to E2-hexenal or solvent (paraffin oil).

C) *Left:* Mean odor-evoked depolarization to each stimulus in B) in the 500 ms after nominal stimulus onset. *Right:* Mean normalized odor-evoked depolarization across all stimuli. Within each stimulus, responses were normalized to the mean odor-evoked depolarization in the solvent-exposed group.
D) Peristimulus time histograms of odor-evoked spiking responses in DL5 PNs from B).
E) *Left:* Mean odor-evoked firing rates to each stimulus from D) in the 500 ms after nominal stimulus onset. *Right:* Mean normalized odor-evoked firing rates across all stimuli, computed analogously as in C).
F) Mean input resistance of DL5 PNs recorded from E2-hexenal- or solvent-exposed flies.
G) Experimental setup for **H-J**). Recordings were established from VM7 PNs that receive direct presynaptic input from the ORN class (pb1a) chronically activated by the rearing odor (2-butanone, 10^{-4}), *n*=6-11 cells.
H-I) As in **B-C**) but describing odor-evoked depolarization in VM7 PNs in response to a concentration series of 2-butanone from flies chronically exposed to 2-butanone or solvent.
J) Mean input resistance of VM7 PNs recorded from 2-butanone- or solvent-exposed flies.
K) Experimental setup for **L-P**). Recordings were established from VA6 PNs that receive direct presynaptic input from the ORN class (ab5a) chronically activated by the rearing odor (geranyl acetate, 10^{-4}), *n*=7-11 cells.
L-P) As in **B-F**) but describing odor-evoked responses to varying concentrations of geranyl acetate in VA6 PNs from flies chronically exposed to geranyl acetate or solvent.
Q-S) Response curves in DL5 **(Q)**, VM7 **(R)**, and VA6 **(S)** PNs from odor-exposed and control flies to a concentration series of the cognate odor for each glomerulus. Results from panels **A-P** are replotted here and extended with measurements at additional stimulus concentrations. *n*=3-19 cells.
All plots are mean ± SEM across flies in each experimental condition. One cell was recorded per fly. Two-tailed p-values report the fraction of resampled absolute differences of means (between simulated experimental groups) which are greater than the absolute observed difference between the means of experimental groups (odor-exposed versus solvent-exposed) (see **Methods**). Starred (*) *p*-values are significant at the level of α=0.05, corrected for multiple comparisons (Bonferroni adjustment). See Supplemental Table 1 for the full genotype and number of cells in every condition.

Figure 2 – source data 1
Source data for Figure 2B-C, 2D-E, 2H-I, 2L-M, 2N-O.

confirmed that E2-hexenal exposure increased odor-evoked firing rates in DL5 PNs to weak, but not strong levels of stimulation (Figure 2E). When firing rates in E2-hexenal exposed flies were normalized to the control rate within each stimulus, we observed an overall increase in odor-evoked DL5 PN firing rate due to E2-hexenal exposure (Figure 2F). Differences in the amount of membrane depolarization between odor- and solvent-exposed groups were not statistically significant at any stimulus concentration (Figure 2C), suggesting a small, but systematic increase in membrane depolarization was nonlinearly amplified by its interaction with the firing threshold in DL5 PNs.

We next asked whether these results generalize to other glomeruli. Using the same approach, we exposed flies to either 2-butanone (10^{-4}), which selectively activates ORNs projecting to glomerulus VM7 (Figure 2G), or geranyl acetate (10^{-4}), which selectively activates ORNs projecting to glomerulus VA6 (Figure 2K). The concentrations of these odors were chosen because each stimulus selectively and reliably elicits high firing rates (>100-150 Hz) in its

corresponding PN, comparable to the level of E2-hexenal (10^{-7}) activation of DL5 PNs. Again, we chronically exposed flies (separate groups) for two days to each of these stimuli and measured the responses in each PN type (corresponding to the glomerulus receiving direct input from the activated ORNs) to a concentration series of each odor (Figure 2G, 2K). Similar to the DL5 glomerulus, VM7 PNs in 2-butanone-exposed flies exhibited modest increases in odor-evoked depolarization to 2-butanone as compared to control flies, and these effects were more pronounced at weak concentrations (10^{-7}) (Figure 2H-I, 2R). VM7 PN spikes are small and filtered in comparison to those of other PNs, and odor-evoked spikes riding on large depolarizations could not be reliably counted across all firing rates in our data set. Therefore, for VM7 PNs only, we report odor responses only in terms of membrane depolarization.

However, chronic activation of direct ORN input to VA6 PNs by exposure to geranyl acetate did not alter PN odor responses across the entire range of concentrations of the familiar odor geranyl acetate, neither at the level of membrane depolarization nor firing rate (Figure 2L-P, 2S). These concentrations elicited levels of membrane depolarization (ranging from 10 to 30 mV) which were similar to that at which other PN types exhibited plasticity after chronic exposure. Together, these results demonstrate that, in some glomeruli like DL5 and VM7, chronic activation of direct ORN input modestly enhanced PN odor responses to weak stimuli, resulting in an overall expansion of the range of stimulus concentrations dynamically encoded by PN activity. However, this effect does not appear to be universal across all glomeruli.

Chronic excitation of ORNs in other glomeruli alters PN response properties

Although olfactory input is compartmentalized into feedforward excitatory channels organized around each glomerular unit, odor processing depends on an extensive network of local neurons (LNs) that mediate lateral excitatory and inhibitory interactions among glomeruli[42]. Thus, PN odor responses reflect both direct input, from its presynaptic ORN partners, and

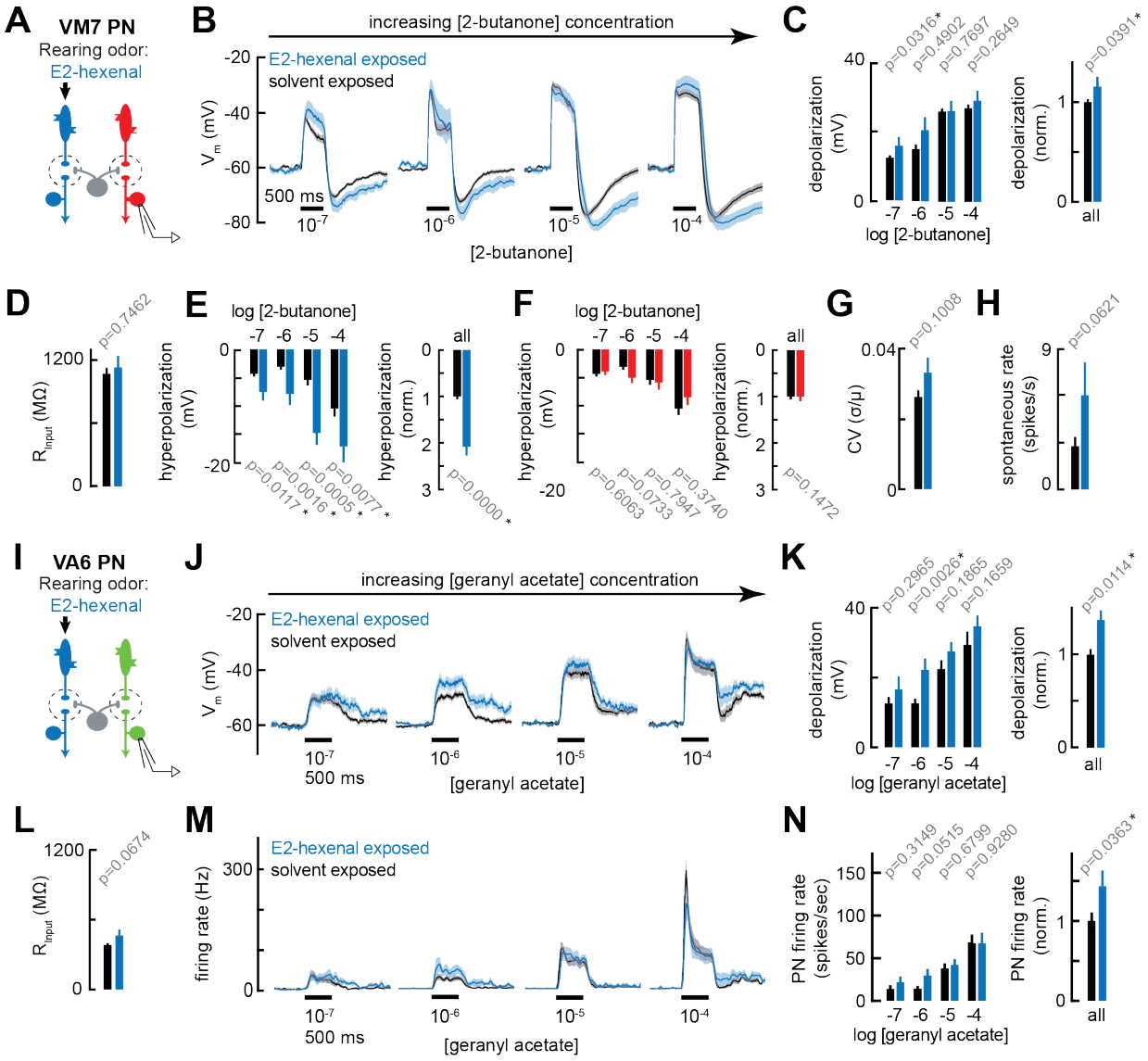

Figure 3: Chronic excitation of ORNs in other glomeruli alters PN response properties.
A) Experimental setup for **B-E**) and **G-H**). Recordings were established from VM7 PNs that receive indirect activity from the ORN class (ab4a) chronically activated by the rearing odor (E2-hexenal, 10^{-7}), *n*=3-11 cells.
B) Odor-evoked depolarization in VM7 PNs in response to varying concentrations of 2-butanone from flies chronically exposed to E2-hexenal or solvent (paraffin oil).
C) *Left:* Mean odor-evoked depolarization to each stimulus from B) in the 500 ms after nominal stimulus onset. *Right:* Mean normalized odor-evoked depolarization across all stimuli. Within each stimulus, responses were normalized to the mean odor-evoked depolarization in the solvent-exposed group.
D) Mean input resistance of VM7 PNs recorded from E2-hexenal- or solvent-exposed flies.
E) *Left:* Mean post-stimulus hyperpolarization in VM7 PN responses to each stimulus from B), calculated over a 2.5 s window after stimulus offset. *Right:* Mean normalized post-stimulus hyperpolarization across all stimuli. Within each stimulus, responses were normalized to the mean post-stimulus hyperpolarization in the solvent-exposed group.
F) Same as **E**), but for VM7 PNs from **Figure 2H** with chronic activation of direct ORN input. Measurements are from VM7 PN recordings in flies chronically exposed to 2-butanone (red) or solvent (black), *n*=6-11 cells.
G) Mean coefficient of variation (CV) of membrane potential in VM7 PNs (from **B**), computed over the 5 s window before stimulus onset, in E2-hexenal- or solvent-exposed flies.
H) Mean spontaneous firing rate of VM7 PNs (from **B**) during the 5 s window before stimulus onset in E2-hexenal- or solvent-exposed flies.

Figure 3 *(continued)*: I) Experimental setup for **J-N**). Recordings were established from VA6 PNs that receive indirect activity from the ORN class (ab4a) chronically activated by the rearing odor (E2-hexenal, 10^{-7}), *n*=5-11.
J-K) As in **B-C**) but for odor-evoked depolarization in VA6 PNs to varying concentrations of geranyl acetate. **L)** As in D) but for VA6 PNs.
M-N) As in **B-C**) but for odor-evoked spiking in VA6 PNs in response to varying concentrations of geranyl acetate (corresponding to J), from flies chronically exposed to E2-hexenal (10^{-7}) or solvent (paraffin oil).
All plots are mean ± SEM across flies, one cell/fly, in each experimental condition. *p*-values are as described in Figure 2. See Supplemental Table 1 for the full genotype and number of flies in every condition.

Figure 3 – source data 1
Source data for Figure 3B-C, 3E-F, 3J-K, 3M-N.

indirect input, arising from activity in other glomeruli and received via local lateral circuitry. Having observed that chronic activation of an ORN class that provides direct input to a PN can elicit some plasticity in that PN, we next asked whether this plasticity is selective for those PNs directly postsynaptic to the chronically active ORNs, or whether PNs that receive only indirect activity from the chronically active ORN subtype are similarly affected. To address this question, we evaluated odor responses in VM7 and VA6 PNs from flies chronically exposed to E2-hexenal (10^{-7}) (Figure 3A, 3I), which provides direct excitation to the DL5 glomerulus.

Chronic indirect excitation evoked plasticity with varying properties in different PNs. In E2-hexenal exposed flies, non-DL5 PNs had mildly enhanced responses to weak stimuli (Figure 3B, 3J). This effect was small but consistently observed in both VM7 and VA6 PNs at the level of odor-evoked depolarization (Figure 3C, 3K). In VM7 PNs, the baseline spontaneous firing rate also trended higher in E2-hexenal exposed flies as compared to controls (Figure 3G-H). Finally, chronic indirect excitation impacted the post-stimulus response properties of some PNs. For example, odor-evoked depolarization in VM7 PNs from E2-hexenal-exposed flies had a more pronounced and prolonged afterhyperpolarization as compared to controls (Figure 3B, 3E), or as compared to flies that experienced chronic direct excitation (2-butanone exposed) (Figure 2H, 3F). This effect does not appear to generalize to all glomeruli. VA6 PNs, for instance, exhibit comparatively different post-stimulus response dynamics, characterized by an epoch of delayed excitation that persists beyond odor offset (Figure 3J). In recordings from VA6 PNs in E2-hexenal exposed flies, this post-stimulus excitation was enhanced across multiple odor concentrations,

as compared to solvent-exposed controls (Figure 3J-K). Most of these differences, however, were within the range of subthreshold depolarizations, and so the overall impact of chronic indirect excitation on VA6 firing rates was mild (Figure 3M-N). Together, these experiments demonstrated that chronic, focal excitation of a single ORN class can lead to changes in PN odor response properties in multiple glomeruli, including in glomeruli not receiving direct synaptic input from the chronically activated ORN class. This result implicates local lateral circuitry in the antennal lobe in activity-dependent PN plasticity after chronic exposure to odor.

Chronic exposure to intense monomolecular odor can affect PN odor responses similarly to chronic exposure at naturalistic concentrations

The divergence of our results so far from those of some past studies, which concluded that chronic odor exposure elicits selective, long-lasting reductions in PN sensitivity[6,8], was surprising. Besides differing in how PN odor responses were measured (electrophysiology versus calcium imaging in past work), the major difference in our study is the odor environment in which flies are reared. Whereas past studies placed the odor source, a vial of concentrated monomolecular odor (1-20%), into the growth environment of the fly, we introduced monomolecular odors at comparatively lower concentrations as intermittent pulses into the growth bottle. Our reasoning was that odors at these lower concentrations still activate their corresponding PN type very strongly but are being presented at a concentration that could reasonably occur in a natural source; thus, the experiment more closely models how an odor overrepresented in a natural environment might impact olfactory function. However, given our unexpected results, we next decided to examine how chronic, sustained exposure to intense monomolecular odor affects PN responses.

We introduced into the growth bottle of the flies a small vial containing either 20% geranyl acetate (>1000-fold more concentrated than in Figure 2K-P) or solvent (control). The opening of

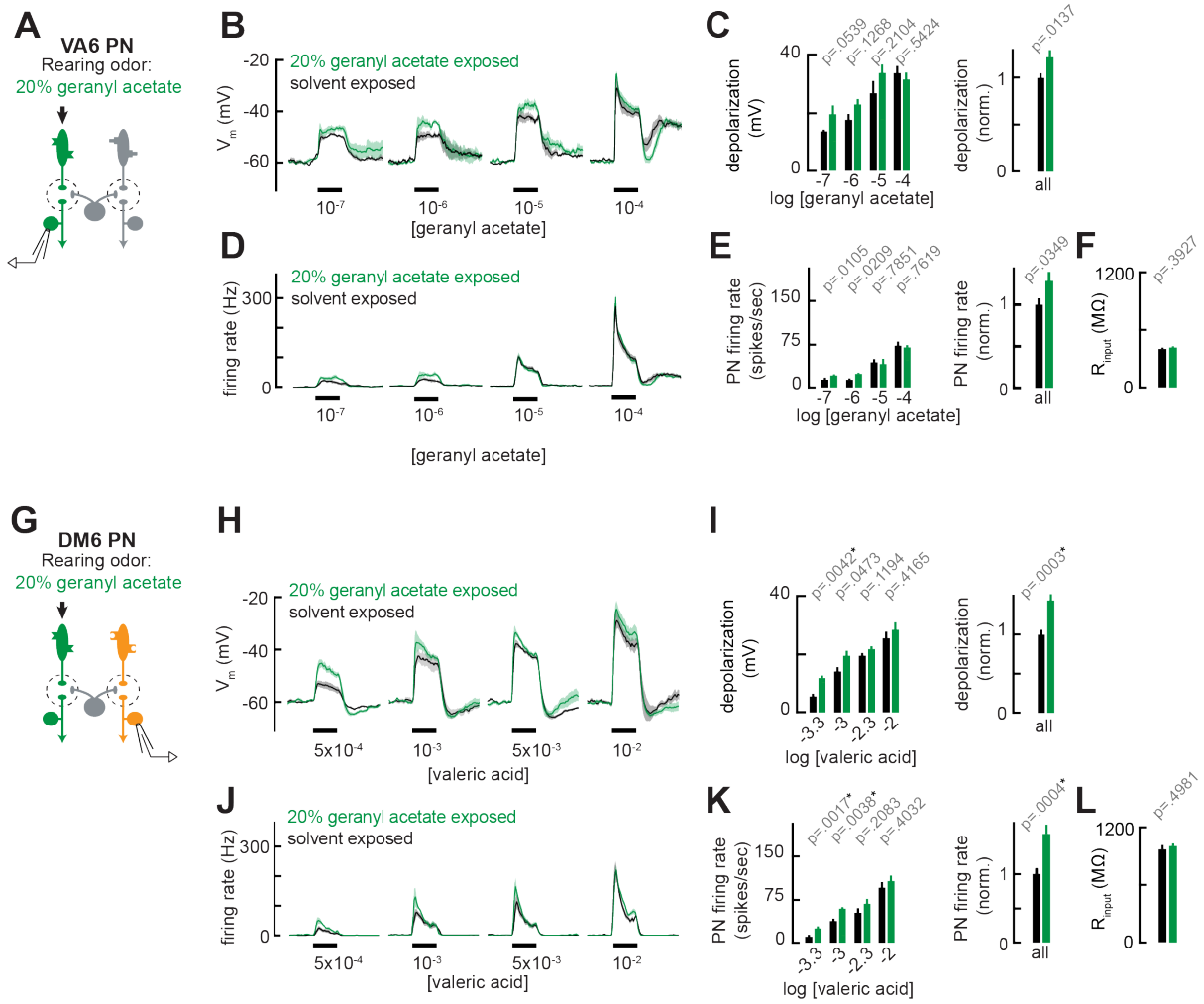

Figure 4: Chronic exposure to intense monomolecular odor can mildly enhance PN responses to weak odor stimuli in PNs that receive either direct or indirect input from chronically active ORNs

A) Schematic of experimental setup for **B-F**. Recordings were established from VA6 PNs receiving direct pre-synaptic input from the ORN class (ab5a) chronically activated by the rearing odor (geranyl acetate, 20%), *n*=5-6.

B) Odor-evoked depolarization in VA6 PNs in response to varying concentrations of geranyl acetate from flies chronically exposed to 20% geranyl acetate or solvent (paraffin oil).

C) *Left:* Mean odor-evoked depolarization to each stimulus in **B)** in the 500 ms after nominal stimulus onset. *Right:* Mean normalized odor-evoked depolarization across all stimuli. Within each stimulus, responses were normalized to the mean odor-evoked depolarization in the solvent-exposed group.

D) Peristimulus time histograms of odor-evoked spiking responses in VA6 PNs from **B)**.

E) *Left:* Mean odor-evoked firing rates to each stimulus from **D)** in the 500 ms after nominal stimulus onset. *Right:* Mean normalized odor-evoked firing rates across all stimuli, computed analogously as in **C)**.

F) Mean input resistance of VA6 PNs recorded from 20% geranyl acetate- or solvent-exposed flies.

G) Experimental setup for **H-L**). Recordings were established from DM6 PNs that receive indirect activity from the ORN class (ab5a)) chronically activated by the rearing odor (geranyl acetate, 20%), *n*=5-6 cells.

H-L) As in **B-F**, but for DM6 PNs in response to varying concentrations of valeric acid from flies chronically exposed to 20% geranyl acetate or solvent (paraffin oil).

Figure 4 – source data 1

Source data for Figure 4B-C, 4D-E, 4H-I, 4J-K

the vial was sealed with fine, porous mesh to prevent flies from contacting the odor but allowing diffusion of the odor out of the vial. We chose to expose flies to 20% geranyl acetate because,

even at high concentrations, this stimulus still preferentially excites VA6 ORNs, whereas other odors like E2-hexenal and 2-butanone strongly activate many different ORN classes as the concentration increases[22,25]. Each group of flies was continuously exposed to 20% geranyl acetate or solvent for four days, as in prior studies, with the odor source replenished daily. Using the same approach as described above, we recorded from PNs directly postsynaptic to ORNs activated by geranyl acetate (VA6, Figure 4A) or PNs that receive indirect input from them (DM6, Figure 4G). We found that chronic, sustained exposure to 20% geranyl acetate had little or no effect on VA6 PN odor responses spanning the range of concentrations of geranyl acetate tested (Figure 4B-F). VA6 PN responses in 20% geranyl acetate-exposed flies consistently trended higher than in solvent-exposed flies, particularly at the level of odor-evoked membrane depolarization (Figure 4B-C), but these small differences were not statistically significant after correction for multiple comparisons. Odor responses in DM6 PNs, which are excited by valeric acid, were moderately increased in 20% geranyl acetate-exposed flies as compared to solvent-exposed control flies (Figure 4H-L). As was the case in our earlier experiments, these heightened responses were most pronounced for weaker odor stimuli (Figure H-K). These results indicate that uninterrupted, chronic exposure to an intense monomolecular odor, 20% geranyl acetate, for four days has only a moderate effect on PN odor coding, qualitatively similar to the impact of long-lasting but intermittent exposure to odors at lower, naturalistic concentrations (Figures 2 and 3). We did not observe reductions in PN olfactory sensitivity in flies reared in any of the four odorized environments we studied. Together, these results show that prior reports indicating that chronic excitation reduces PN sensitivity do not, at a minimum, hold true for all glomeruli. In all cases we examined – DL5, VM7, and VA6 – the overall effect of chronic odor stimulation was limited to either no change or small increases in PN sensitivity, with the effects of olfactory plasticity most significant for the encoding of weak odor stimuli.

PN coding of odor mixtures is unaffected by chronic odor exposure

So far, we have evaluated PN odor responses using monomolecular odor stimuli, chosen because some activate only a single ORN class when presented at lower concentrations. We began with this approach so that the presynaptic source of odor-evoked input with respect to each PN type was unambiguous; however, typical odors activate multiple ORN classes[21,22]. Thus, we next investigated how chronic odor exposure impacts the coding of typical odor stimuli that elicit mixed direct and indirect synaptic input to PNs.

As before, we recorded from VM7 PNs in flies chronically exposed to E2-hexenal (10^{-7}), 2-butanone (10^{-4}), or solvent (Figure 5A, D). We mixed a fixed concentration of pentyl acetate (10^{-3}), a broadly activating odor that drives activity in many ORN types (but does not activate pb1a, the VM7 ORN), with increasing concentrations of 2-butanone, the odor that elicits direct activity in VM7[24,43]. Overall, blending pentyl acetate with 2-butanone reduced VM7 PN responses, as compared to their response to 2-butanone alone (Figure 5B, 2H and Figure 5E, 3B). Such mixture inhibition is well understood to be a consequence of lateral GABAergic inhibition elicited by activity in non-VM7 ORNs[24,44]. Whereas responses of VM7 PNs to direct excitation (driven by 2-butanone) were modestly enhanced in 2-butanone exposed flies (Figure 2H-I), VM7 responses to mixed direct and indirect input (driven by blends of 2-butanone and pentyl acetate) were similar in control and 2-butanone exposed flies (Figure 5B-C). This effect was observed across a wide range of concentrations of 2-butanone, each blended with a fixed concentration of pentyl acetate. Similar results were observed when we recorded odor mixture responses from VM7 PNs in E2-hexenal exposed flies (Figure 5D), which received chronically elevated indirect activity. Whereas chronic exposure to E2-hexenal altered VM7 PN responses to 2-butanone (Figure 3B-C, 3E), VM7 PN responses to odor mixtures of 2-butanone and pentyl acetate were indistinguishable between E2-hexenal and solvent-exposed flies (Figure 5E-F). These observations suggest that lateral inhibition may also be impacted by chronic odor exposure,

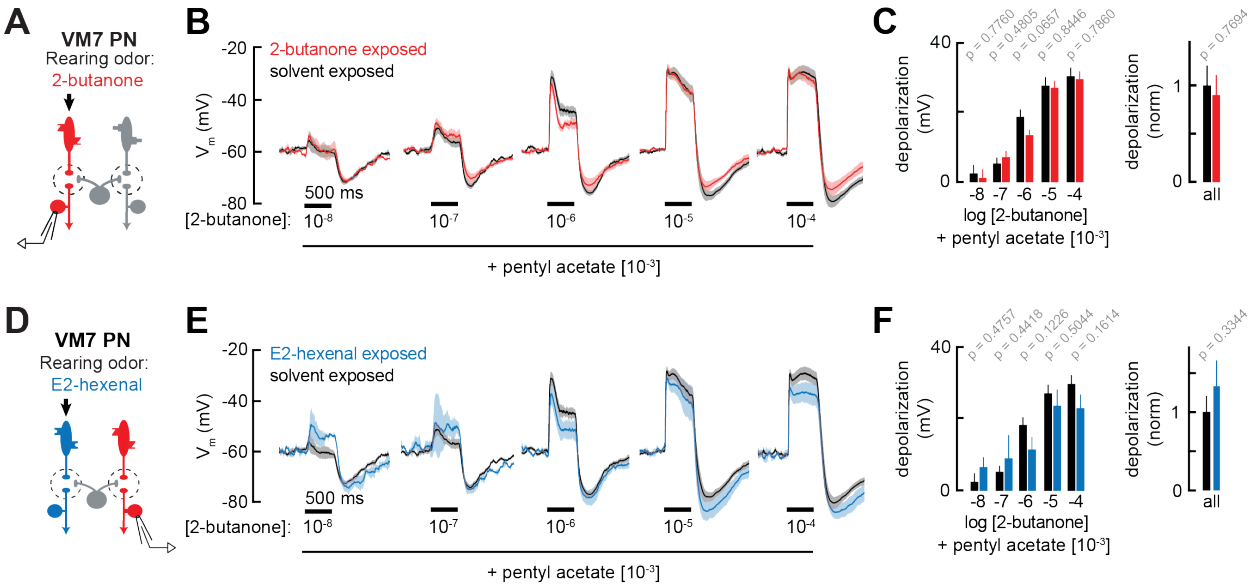

Figure 5: PN responses to odor mixtures are unaffected by chronic activation of direct or indirect ORN inputs.
A) Experimental setup for **B-C)**, which is the same as in Figure **2G-J**. Recordings were established from VM7 PNs that receive direct input from the ORNs (pb1a) chronically activated by the rearing odor (2-butanone, 10^{-4}), *n*=3-7 cells.
B) Odor-evoked depolarization in VM7 PNs from 2-butanone- or solvent-exposed flies to binary mixtures comprised of increasing levels of 2-butanone (10^{-8} through 10^{-4}) blended with a fixed concentration of pentyl acetate (10^{-3}).
C) *Left:* Mean odor-evoked depolarization to each stimulus in B) in the 500 ms after nominal stimulus onset. *Right:* Mean normalized odor-evoked depolarization across all stimuli. Within each stimulus, responses were normalized to the mean odor-evoked depolarization in the solvent-exposed group.
D) Experimental setup for **E-F)**, which is the same as in Figure **3A-E**. Recordings were established from VM7 PNs which receive indirect activity from the ORNs (ab4a) chronically activated by the rearing odor (E2-hexenal, 10^{-7}), *n*=3-7 cells.
E-F) Same as in **B-C**), but for VM7 PNs from E2-hexenal or solvent-exposed flies.
All plots are mean ± SEM across flies (one cell/fly) in each experimental condition. *p*-values are as described in Figure 2. See Supplemental Table 1 for the full genotype and number of flies in every condition.

Figure 5 – source data 1
Source data for Figure 4B-C, 4E-F.

such that odor-evoked input elicits more inhibition to counter modest increases in PN excitation. In this way, stable PN responses are maintained to most typical odors which activate many ORs.

When we examined the anatomy of the LN network, however, we observed that it was not grossly affected by chronic odor exposure. Levels of innervation of individual olfactory glomeruli by the neurites of large subpopulations of inhibitory local neurons (iLNs) (measured as the ratio of iLN neurites to total synaptic neuropil) were largely unchanged by chronic odor exposure (Figure 5 – figure supplement 1A-C). Unexpectedly, in flies chronically exposed to E2-hexenal only, many glomeruli tended to be smaller in volume than their counterparts in solvent-

exposed flies (Figure 5 – figure supplement 1E, G). Similar trends, however, were not observed in parallel experiments where flies were chronically exposed to 2-butanone (Figure 5 – figure supplement 1D). Thus, chronic exposure to some, but not all, odors can elicit mild anatomical perturbations in the olfactory circuit. In contrast with previous reports[6,8,35], however, under our odor exposure conditions, changes in glomerular volume were not glomerulus-specific, but extended globally beyond the chronically active glomerulus.

Chronic activation of ORNs does not alter their odor response properties

Prior studies have suggested that chronic odor exposure increases the sensitivity of ORNs[45,46]. We wondered if, in flies chronically exposed to some odors, heightened PN responses to weakly activating stimuli (which elicit little lateral inhibition) might stem directly from changes in ORN activity. Heightened ORN sensitivity in odor-exposed flies might not be apparent in PN responses to stronger odors if circuit mechanisms such as lateral inhibition, which grow with stimulus strength, were acting to compensate changes in feedforward excitation.

To evaluate how chronic odor exposure affects ORN sensitivity, we exposed flies to E2-hexenal (10^{-7}) or 2-butanone (10^{-4}) as before and recorded extracellular activity from the ORN classes selectively activated by each odor stimulus (Figure 6A, 6D; see Methods). We observed that chronic activation of either ORN type – ab4a ORNs in E2-hexenal exposed flies or pb1a ORNs in 2-butanone exposed flies – did not significantly impact spontaneous (Figure 6 – figure supplement 1E-G) or odor-evoked firing rates across a wide range of stimulus concentrations (Figure 6B-C, 6E-F, Figure 6 – figure supplement 1A-B), including those lower concentrations which elicited enhanced responses in postsynaptic DL5 or VM7 PNs (Figure 2B-E, 2H-I). In addition, we evaluated pb1a ORN (presynaptic to VM7) responses in E2-hexenal exposed flies (Figure 6G) because VM7 PN responses to odor were enhanced in this condition compared to controls (Figure 3B-C). These experiments showed that pb1a odor responses were largely

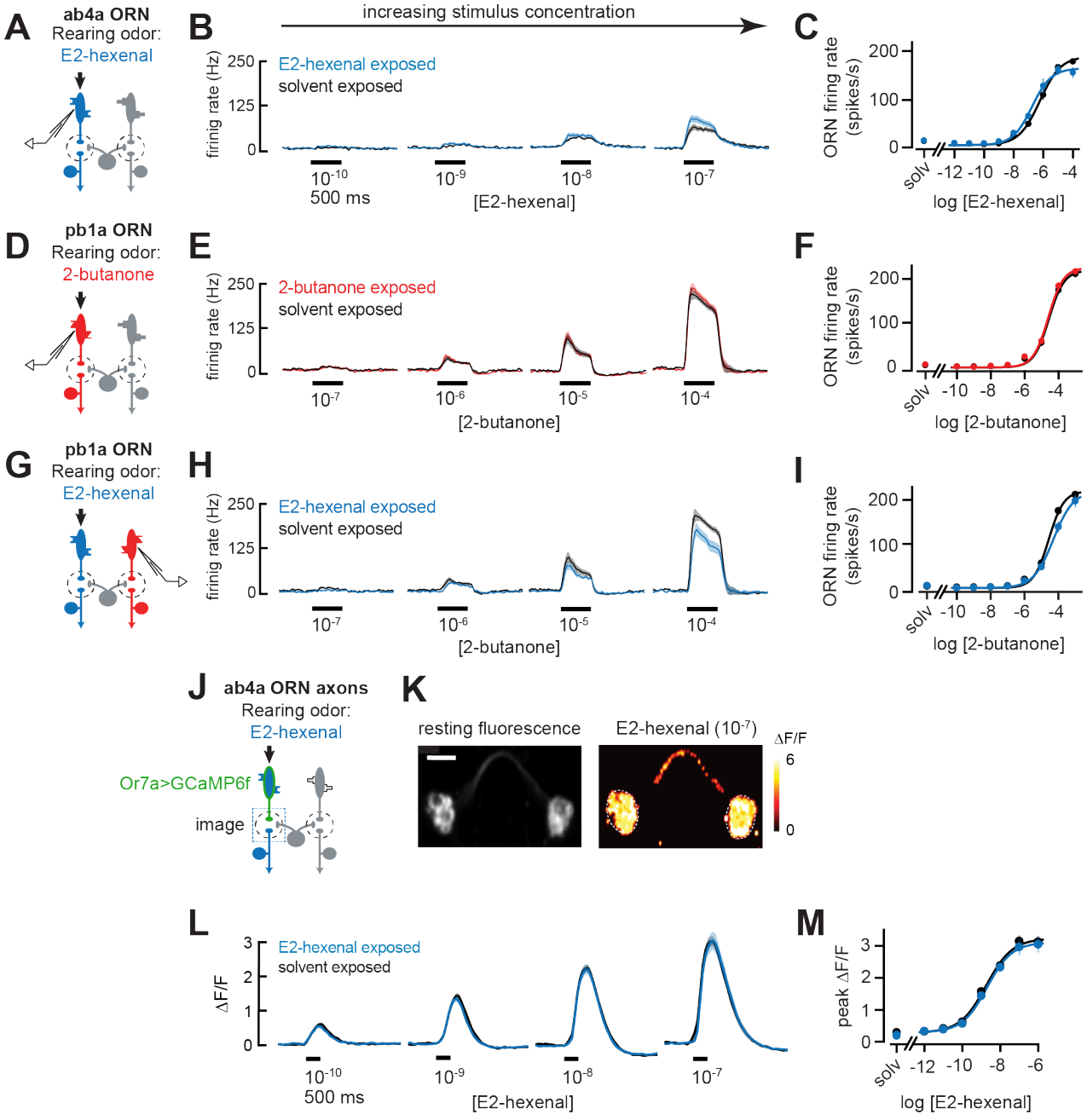

Figure 6: Odor responses in ORNs are unaffected by chronic odor exposure.
A) Experimental setup for **B-C)**. Single-sensillum recordings (SSR) were established from ab4a ORNs, which are directly excited by the rearing odor E2-hexenal (10^{-7}), *n*=6-12 cells.
B) Peristimulus time histograms of odor-evoked spiking in ab4a ORNs in response to varying concentrations of E2-hexenal from flies chronically exposed to E2-hexenal or solvent (paraffin oil).
C) Response curve of mean baseline-subtracted ab4a firing rates (calculated over the 500 ms window of stimulus presentation) to varying concentrations of E2-hexenal in E2-hexenal- or solvent-exposed flies. The concentration-response curve includes responses from **B)**, as well as measurements at additional stimulus concentrations. solv, solvent (paraffin oil).

D) Experimental setup for **E-F)**. SSR recordings from pb1a ORNs, which are directly excited by the rearing odor 2-butanone (10^{-7}), *n*=6-11 cells.
E-F) Same as **B-C)**, but for pb1a ORNs responding to varying concentrations of 2-butanone in flies chronically exposed to 2-butanone or solvent.
Figure 6 *(continued)*: G) Experimental setup for **H-I)**. SSR recordings from pb1a ORNs in flies chronically exposed to E2-hexenal (10^{-7}), a stimulus which directly excites ab4a ORNs, *n*=5-11 cells.
H-I) Same as **B-C)**, but for pb1a ORNs responding to varying concentrations of 2-butanone in flies chronically exposed to E2-hexenal or solvent.
J) Experimental setup for **K-M)**. GCaMP6f was expressed in ab4a ORNs under the control of *or7a-Gal4*. Flies were chronically exposed to E2-hexenal (10^{-7}) or solvent, and odor-evoked calcium responses in ab4a ORN terminals were imaged in the DL5 glomerulus (dashed box) using two-photon microscopy, *n*=6-8 cells.
K) *Left:* Maximum intensity projection of the imaging plane across the time series of an example stimulus presentation. *Right*: Peak $\Delta F/F$ heat map from a single experiment evoked by a 500 ms pulse of E2-hexenal (10^{-7}) in a solvent-exposed fly, averaged across three stimulus presentations. Scale bar is 5 μm.
L) Time courses of change in fluorescence in ab4a ORN terminals elicited by varying concentrations of E2-hexenal in E2-hexenal- and solvent-exposed flies.
M) Response curve of mean peak $\Delta F/F$ responses to varying concentrations of E2-hexenal in E2-hexenal- or solvent-exposed flies. The concentration-response curve includes responses from L), as well as measurements at additional stimulus concentrations. solv, solvent.
All plots are mean ± SEM across flies in each experimental condition (one cell or antennal lobe/fly). Statistical analysis was as in Figure 2 (see **Figure 6 – figure supplement 1** for p-values); none of the comparisons in **Figure 6** between odor- and solvent-exposed groups are statistically significant at the α=0.05 level, with Bonferroni adjustment for multiple comparisons. See Supplemental Table 1 for the full genotype and number of flies in every condition.

Figure 6 – source data 1
Source data for Figure 6B-C, 6E-F, 6H-I, 6L-M.

unaffected by E2-hexenal exposure (Figure 6H-I). Although we observed a small decrease in response to 2-butanone at a concentration of 10^{-4}, this difference did not consistently trend at nearby concentrations (10^{-5} or 10^{-3}) and did not reach statistical significance after correction for multiple comparisons (Figure 6- figure supplement 1C).

We next considered the possibility that small changes in ORN firing rate might not be resolvable in extracellular recordings from individual neurons, but that the high convergence of ORNs onto PNs could amplify small differences in ORN firing into a measurable increase in PN response. Therefore, we used functional imaging to measure the population response of all ab4a ORNs in the DL5 glomerulus (Figure 6J-K), where the axon terminals of dozens of ab4a ORNs[47] converge in a small physical volume (~200 μm^3). We expressed the genetically encoded calcium indicator GCaMP6f in ab4a ORNs under the control of the Or7a-Gal4 promoter. We then chronically exposed these flies to either E2-hexenal or solvent and used two-photon microscopy to record odor-evoked ORN calcium signals in the DL5 glomerulus (Figure 6K). We found that population imaging of ORN terminals had comparatively higher sensitivity for detecting odor

responses, demonstrated by the ability to resolve odor-evoked activity in ab4a ORNs in response to E2-hexenal at a concentration of 10^{-10} (Figure 6L-M), responses which are not detectable by extracellular recordings from individual ORNs (Figure 6B-C). However, functional imaging showed that odor-evoked responses in ab4a ORN terminals in glomerulus DL5 were indistinguishable between E2-hexenal exposed and control flies across the entire range of odor concentrations tested (Figure 6L-M, Figure 6- figure supplement 1D). Taken together, these results indicate that ORN odor responses are unaffected by perturbations in the odor environment that drive over a million additional spikes in each ORN over the course of two days of exposure. They also imply that the PN plasticity we observe likely stems from central cellular or circuit mechanisms, rather than from changes at the periphery.

The role of central circuit mechanisms in olfactory plasticity

We next investigated several central mechanisms that might contribute to olfactory plasticity. First, we asked whether chronic odor exposure changes the intrinsic cellular excitability of PNs. Comparisons of the input resistance of PNs recorded in odor-exposed and control flies showed that postsynaptic input resistance was unaltered by chronic exposure to any of the odors in our study, regardless of odor concentration or whether PNs received direct or indirect chronic activation (Figures 2F, 2J, 2P, 3D, 3L, 4F, 4L). Consistent with these observations, *f-I* curves directly measuring the firing rate of deafferented DL5 PNs in response to current injection at the soma (Figure 7A) were indistinguishable between control and E2-hexenal exposed flies (Figure 7B-C; see also Figure 7 – figure supplement 1A-B). These results indicate that the intrinsic excitability of PNs is unaltered by chronic odor exposure and does not account for the increase in PN sensitivity to weak odors.

Next, we asked whether ORN-PN synaptic strength is impacted by chronic odor exposure. In each glomerulus, many axon terminals from the same ORN class synapse onto

each uniglomerular PN, and each ORN communicates with each PN via multiple active zones[48–51]. We refer to the combined action of all the neurotransmitter release sites between a single ORN and a PN as a unitary ORN-PN synapse. To measure the strength of a unitary synaptic connection between ab4a ORNs and DL5 PNs, we adapted a previously established minimal stimulation protocol[49] for use with optogenetic-based recruitment ORN activity. We expressed the channelrhodopsin variant Chrimson[52] in all ab4a ORNs, driven from the Or7a promoter[17], acutely severed the antennal nerve, and stimulated ORN terminals with wide-field light delivered through the imaging objective. Concurrently, we monitored synaptic responses in DL5 PNs using targeted whole-cell recordings in voltage clamp mode (Figure 7D).

We employed a minimal stimulation protocol to isolate unitary excitatory postsynaptic currents (uEPSCs) evoked by single presynaptic ORN spikes. Stimulation with very low levels of light elicited no synaptic response in the PN (Figure 7E). As the power density was gradually increased, trials of mostly failures were interspersed with the abrupt appearance of an EPSC in an all-or-none manner. Further ramping the light in small increments had no effect on the amplitude of the EPSC in the PN, until a power density was reached where the EPSC amplitude abruptly doubled, as compared to the amplitude of the initially recruited EPSC (Figure 7E). Light-evoked EPSCs were dependent on providing flies with the rhodopsin chromophore all-trans-retinal (ATR) in their food; PNs from flies raised on non-ATR supplemented food displayed no light-evoked responses (data not shown). The step-like profile of EPSC amplitudes as a function of power density likely reflects the discrete recruitment of individual ORN axon fibers with increasing stimulation. In particular, the sharp transition from mostly failures to a reliably evoked current is consistent with the response arising from the activation of a single ORN input. The time from the onset of light stimulation to the evoked uEPSC was variable and averaged approximately ~23 ms $\pm$ 2.2 ms (s.d.) (Figure 7- figure supplement 1C), similar to the distribution of latencies to the first light-evoked ORN spike at comparable intensities (data not shown[53]).

385

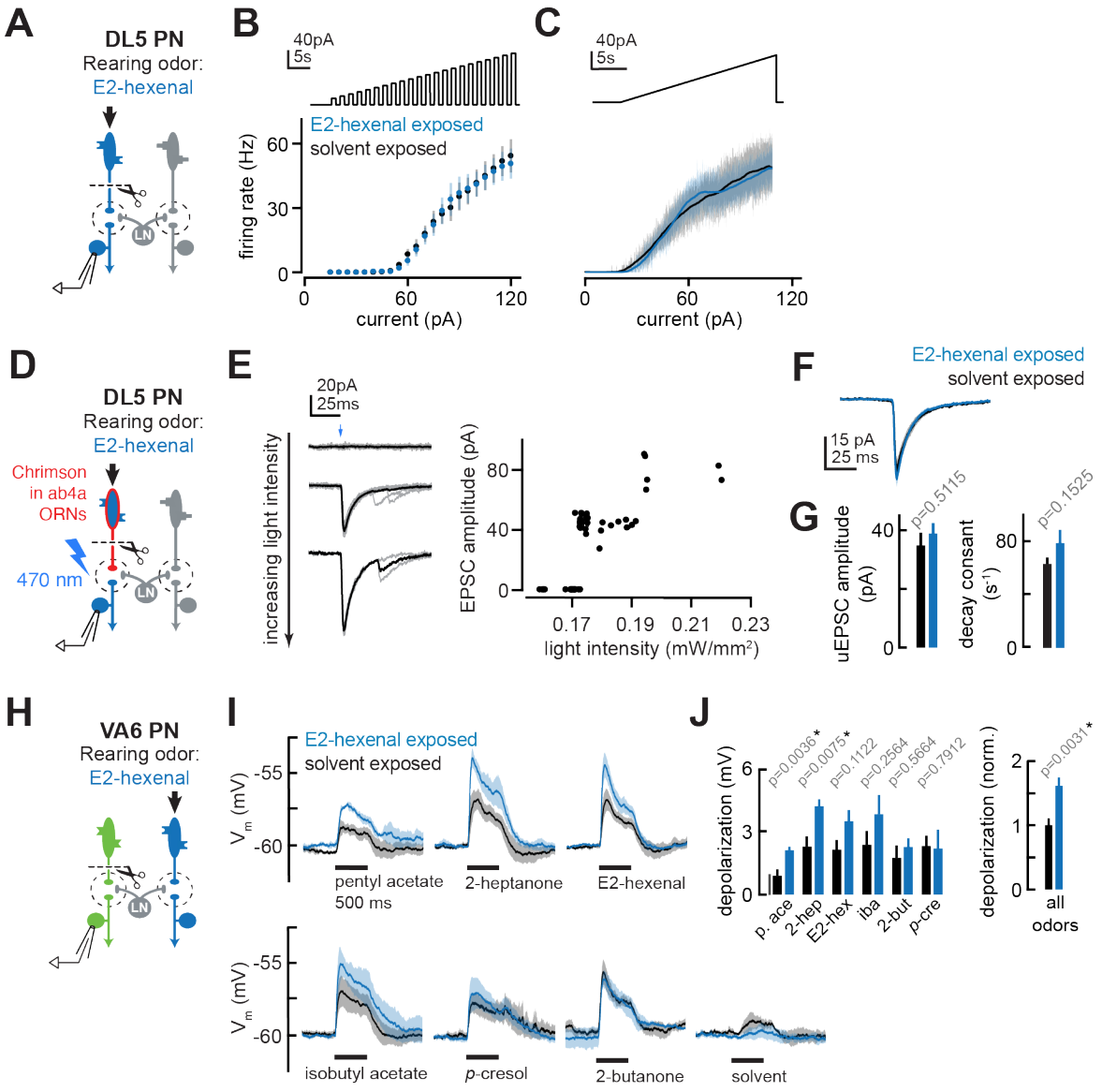

Figure 7: The effect of chronic ORN activation on PN intrinsic properties, ORN-PN synapse strength, and lateral excitation in the antennal lobe.

A) Experimental setup for **B-C)**. Recordings were established from DL5 PNs, which receive direct presynaptic input from the ORN class (ab4a) chronically activated by the rearing odor (E2-hexenal, 10^{-7}), *n*=4 cells. Immediately prior to recording, PNs were deafferented by bilateral transection of the antennal nerves.

B) *f-I* curve of DL5 PNs from E2-hexenal- and solvent-reared flies plotting firing rates elicited by increasing levels of current injection (1 s pulses delivered at an interpulse interval of 1 s and increasing with a step size of 5 pA).

C) Same as **B)** but plotting firing rates elicited by injection of a slow triangular current ramp (4.5 pA/s). Firing rate was calculated in 50ms bins with 25 ms overlap.

D) Experimental setup for measurement of synaptic strength between ab4a ORNs and DL5 PNs in **E-G)**. Flies expressing the channelrhodopsin CsCrimson in ab4a ORNs under the control of *or7a-Gal4* were chronically exposed to E2-hexenal (10^{-7}) or solvent. Immediately prior to the experiment, PNs were deafferented by bilateral transection of

the antennal nerves. Recordings were established from DL5 PNs, and unitary EPSCs were elicited in PNs by light-based minimal stimulation of presynaptic ORN terminals. *n*=5-7 cells.

E) A minimal stimulation protocol recruits unitary EPSCs. *Left*: EPSCs recorded in a DL5 PN (from a solvent-exposed fly) in response to increasing levels of light-based (488 nm) ORN stimulation (blue arrow). Individual trials are in grey; the average of all trials at a given light intensity is in black. *Right*: EPSC amplitude as a function of light intensity. Each dot represents the peak EPSC amplitude from a single trial. As light intensity is gradually increased, an evoked EPSC

Figure 7 *(continued)*: appears abruptly, and its amplitude remains constant as the light intensity is further increased. This range (~0.17-0.19 mW/mm^2) likely corresponds to recruitment of an action potential in a single ab4a ORN axon presynaptic to the DL5 PN. As the level of light driven ORN stimulation further increases, the amplitude of the evoked EPSC suddenly doubles, likely reflecting the recruitment of a second axon.

F) Mean unitary EPSC recorded in DL5 PNs from E2-hexenal- or solvent-exposed flies.

G) Mean unitary EPSC amplitude (left) and decay rate (right) in DL5 PNs from E2-hexenal- or solvent-exposed flies.

H) Experimental setup for **I-J)**. Recordings were established from VA6 PNs in flies chronically exposed to E2-hexenal or solvent. Immediately prior to recording, PNs were deafferented by bilateral transection of the antennal nerves. Odors stimulate intact ORNs located in the palps and recruit lateral input to VA6 PNs (which normally receive direct input from ORNs in the antenna). *n*=3-5 cells.

I) Odor-evoked depolarization in deafferented VA6 PNs elicited by the indicated stimuli in flies chronically exposed to E2-hexenal or solvent (paraffin oil). Odors were presented at 10^{-2} dilution.

J) *Left:* Mean odor-evoked depolarization to each stimulus in **I)** in the 500 ms after nominal stimulus onset. *Right:* Mean normalized odor-evoked depolarization across all stimuli. Within each stimulus, responses were normalized to the mean odor-evoked depolarization in the solvent-exposed group.

All plots are mean ± SEM across flies in each experimental condition (one cell/fly). *p*-values are as described in **Figure 2**. See Supplemental Table 1 for the full genotype and number of flies in every condition.

Figure 7 – source data 1
Source data for Figure 7B-C, 7F-G, 7I-J.

Using this optogenetic-based ORN recruitment method, the amplitude (~40 pA), rise time (~2 ms), and half decay time ($t_{1/2}$ ~ 7ms) of uEPSCs in DL5 PNs (Figure 7F) in the control condition were similar to previous measurements made using conventional electrical stimulation of the antennal nerve[49], confirming this method for measuring unitary ORN-PN synapse properties.

We used this method to record uEPSCs from DL5 PNs in flies chronically exposed to either solvent or E2-hexenal (10^{-7}), the odor which directly activates the presynaptic ORNs. To compare recordings across different trials, individual uEPSCs from each condition were aligned by their peaks and averaged. Average DL5 uEPSC amplitudes and response kinetics were indistinguishable between solvent and E2-hexenal exposed flies (Figure 7F-G). This result shows that ORN-PN strength is unchanged by chronic odor exposure and is unlikely to account for enhanced DL5 PN responses to weak stimuli in E2-hexenal exposed flies.

Finally, we considered the possibility that local lateral excitatory connections play a role in PN plasticity triggered by chronic odor exposure. Olfactory glomeruli in the antennal lobe are densely interconnected by a network of lateral excitatory local neurons (eLNs) that signal globally

via electrical synapses to boost PN excitability[54–57]. The effects of lateral excitation on PN responses are most significant in the regime of weak odor stimuli[56,57]. Lateral excitatory input to PNs is most directly measured by removing the source of direct input to the PN and recording PN activity while stimulating ORNs that directly excite other glomeruli[54–56]. The fly has two sets of olfactory organs – the antennae and the palps – and each ORN class resides in one or the other, but never both. We chronically exposed files to either solvent or E2-hexenal (10^{-7}), bilaterally removed the antennae, and established recordings from VA6 PNs while stimulating the palps with odor (Figure 7H). Since VA6 PNs receive direct input from ORNs located in the antenna, VA6 PN odor responses recorded in this configuration stem from lateral (indirect) input that originates from ORNs located in the palp.

The stimulus panel for this experiment was comprised of odors that broadly activate many ORN classes, including those housed in the palps. As previously shown[54,57], different odors elicit differing, but characteristic amounts of lateral excitation in VA6 PNs (Figure 7I). Many, but not all, odors evoked increased lateral excitation in VA6 PNs from E2-hexenal exposed flies, as compared to solvent-exposed flies(Figure 7I-J). To pool our measurements of lateral excitatory responses in VA6 PNs across stimuli, we normalized the amount of PN membrane depolarization elicited by each odor in E2-hexenal exposed flies to the average amount it elicited in solvent-exposed flies. This analysis confirmed that the average amount of odor-evoked lateral excitation across all stimuli was increased in E2-hexenal exposed flies, as compared to solvent-exposed controls (Figure 7J). These results suggest that chronic odor exposure increases the overall strength of global excitatory coupling among glomeruli in the antennal lobe after chronic odor exposure, which may contribute to the heightened sensitivity of PNs to weak odors.

DISCUSSION

We found that strong, persistent activation of a single class of olfactory receptor neurons triggers only limited plasticity at early stages of olfactory processing in *Drosophila*. Chronic exposure to monomolecular odors at concentrations that can be found in the natural world elicited modest increases in the olfactory sensitivity of some PNs. Qualitatively similar effects on PN odor coding were observed even when exposing flies to high concentrations of a monomolecular odor, geranyl acetate. When present, experience-dependent plasticity in PNs mostly affected the encoding of weak odor stimuli, whereas responses to stronger odors, which more strongly recruit local inhibition, were largely unaffected. Many elements of the antennal lobe circuit, including ORN sensitivity, PN intrinsic properties, and ORN-PN synapse strength, were unaffected by chronic ORN activation. Plasticity triggered by chronic ORN activity was observed not only in PNs corresponding to the glomerulus that receives direct input from the chronically active ORNs, but also in PNs corresponding to other glomeruli, indicating that experience-dependent plasticity in PNs is not glomerulus- or odor-specific. This result implicates lateral interactions between glomeruli as having a role in olfactory plasticity, consistent with our observation that odor exposure can boost the level of lateral excitatory coupling between some PNs. Thus, even in odor environments that elicit unusually high, long-lasintg levels of activity in a single ORN class, the representation of odors in the antennal lobe is mostly stable. Chronic odor stimulation results in either no or mild changes in PN responses, which sensitize PNs to weak stimuli and extend the lower range of stimulus intensities dynamically encoded by the PN. Reduced PN responses were not observed in response to chronic excitation in any condition we tested, inconsistent with the hypothesis that PN olfactory codes adjust to the frequency with which specific odors are encountered in the environment.

Chronic exposure to odors elicits limited plasticity in PN odor responses

Chronic activation of at least two ORN classes by odors at naturalistic concentrations elicited modest increases in the odor sensitivity of the cognate PNs (DL5 and VM7) receiving direct presynaptic input from each. A third PN type (VA6) was unaffected by exposure to lower naturalistic concentrations of odor (Figure 2). These results contrast with prior studies in flies in which chronic exposure to monomolecular odors delivered at high concentrations selectively reduced the sensitivity of PNs activated by these odors[6,8]. We considered the possibility that exposure to higher concentrations of odor was necessary to elicit PN plasticity; however, we found that chronic sustained exposure to high concentrations of geranyl acetate (from a 20% v/v source) had a similar effect on VA6 PN odor responses as exposure to geranyl acetate at more than a 1000-fold lower concentration. This result is expected because VA6 PNs are near maximally activated (~300 Hz peak firing rate) at the naturalistic concentration (10^{-4}) used, and further increasing the concentration of odor does not drive substantially more activity in VA6 PNs. These findings show that the commonly accepted idea that chronic odor exposure reduces the sensitivity of PNs processing the familiar odor is, at the very least, not true for all odors and glomeruli.

Establishing the direction of olfactory plasticity evoked in response to elevated levels of olfactory input seems important, as it would point towards differing functional consequences of plasticity for olfactory coding. Consistent with our results, another study observed that sustained, chronic exposure of flies to 1% geranyl acetate weakly enhanced VA6 PN responses[38], though this study evaluated a single odor at a single concentration, so the generality of the result was unclear. Another analogous study in mice found that odor-evoked mitral cell activity in the olfactory bulb was modestly increased after chronic odor exposure to intense monomolecular odors[28]. Both studies measured odor-evoked activity using functional calcium imaging, suggesting that the use of electrophysiology to measure olfactory activity in our study does not account for the difference in outcomes. Since methodological details differ between

any two studies, we do not know whether chronic odor stimulation can reduce PN sensitivity in some specific contexts. For instance, we cannot rule out the possibility that chronic excitation of different glomeruli has different outcomes, such that PN sensitivity is adjusted according to specific rules useful for each individual odor and glomerulus. Much of the prior work has focused on the V glomerulus, which processes the important environmental cue carbon dioxide and could be subject to a different form of plasticity. Because of the position of PN cell bodies in the antennal lobe, evaluating V PN odor responses using whole-cell recordings is technically challenging. However, in PNs corresponding to the three different glomeruli we did study, each activated by different odors, chronic excitation was consistently observed to boost responses to weak odors in most cases, and reduced PN responsiveness was never observed.

The use of low, naturalistic odor concentrations for studying olfaction

In this study, flies were exposed to periodic one-second pulses of odor at estimated concentrations of ~10 ppb to ~10 ppm in air (see Methods). Though the overrepresented odor narrowly activated a single olfactory channel, it was delivered to flies living in an active culture containing cornmeal food, yeast, and other flies. As such, the olfactory circuit is expected to be broadly active during the period of chronic odor exposure. Our goal with this experimental design was to drive a robust difference in levels of neural activity in a single ORN type compared to control animals, while still maintaining animals in an olfactory environment that could be plausibly encountered in the natural world.

Nearly all prior studies investigating olfactory plasticity, in flies or rodents, chronically excite the olfactory system using odors delivered at comparatively higher concentrations, generally ranging from ~10^3 to ~10^5 ppm in air [6,8,28,35,39,58]. Such stimuli are unlikely to be found in natural odor sources; for comparison, headspace concentrations of the most abundant small ester, alcohol, and aldehyde volatiles common in fruit odor sources typically range from ~1 ppb

to ~10 ppm in air (for examples, see[59–61]). Indeed, for many volatile organic compounds, prolonged exposure at concentrations that exceed ~10^3 ppm is considered hazardous to human life or health (NIOSH[62]). Since rates of odor-evoked firing in many olfactory neurons are saturated at concentrations well below these intense concentrations, it may be preferable, when possible, to use odor stimuli within the concentration range likely to be encountered in the natural evolutionary history of the animal. However, we note that, though it was not the subject of this study, understanding how exposure to very intense odors impacts olfactory behavior and function is an important priority, since both animals and humans frequently encounter such situations in modern industrialized environments[63–65].

Stimulus-selective versus global plasticity in sensory circuits

Another important difference between our results and some prior work is that the mild olfactory plasticity we observed did not selectively occur only in the glomerulus receiving direct input from the chronically activated ORN class. Some prior studies showed that the effects of chronic odor exposure on olfactory neuron responses and anatomical volume affect only specific glomeruli, although the direction of these effects varied between studies[6,8,35,36,45]. Most studies exposed flies to odors that broadly activate many ORN classes, complicating the interpretation of the degree of selectivity of olfactory plasticity. In cases where flies were exposed to an intense monomolecular odor that excited a single ORN class, for instance, CO_2-sensitive ORNs that project to the V glomerulus, olfactory responses of PNs receiving direct and indirect chronic excitation were not directly compared[6,8]. Determining the degree to which PN plasticity is stimulus- and glomerulus-specific is significant because it affects the extent to which PN plasticity can account for stimulus-specific changes in olfactory behavior after chronic exposure, as well as whether PN plasticity can reshape the olfactory code to reflect the distribution of specific odors in the environment.

This study rigorously tested this hypothesis by growing animals in odor environments that selectively increased olfactory activity in a single ORN class, and then evaluating the olfactory sensitivity of PNs that receive either direct or indirect activity from the chronically excited ORNs. Under our experimental conditions, we found that olfactory plasticity is non-selective and occurs broadly in many glomeruli. Chronic ORN excitation could trigger mild increases in odor responses both in PNs receiving direct excitation and PNs receiving indirect excitation form the chronically active ORN class.

Plasticity elicited by chronic indirect input did not impact all PNs equivalently. For example, chronic elevation of indirect input to VM7 PNs (by exposure to E2-hexenal) mildly increased VM7 PN sensitivity and also significantly increased levels of post-stimulus hyperpolarization in the cell. However, this latter effect was not observed in VA6 PNs, nor in DM6 PNs in flies exposed to 20% geranyl acetate, which exhibited normal post-stimulus dynamics (Figure 3B, 3J). These results suggest that olfactory plasticity differentially impacts PNs in different glomeruli, possibly due to how the circuit mechanisms underlying plasticity interact with the varying intrinsic biophysical characteristics of each PN type.

Our observation that chronic olfactory stimulation broadly affects many PN types is similar to that of a recent functional imaging study in mouse which found that chronic odor exposure in early postnatal life induced widespread, global enhancement of mitral cell excitability across the olfactory bulb[28]. Chronic, persistent olfactory activity may function to adjust the overall gain or sensitivity of the circuit, especially in the weak stimulus regime. Such a widespread increase in excitability might reflect a form of generalized sensory enrichment that has been previously described in mammalian olfactory[66,67], visual[68,69], and auditory[70] systems .

Mechanisms of olfactory plasticity in the antennal lobe

PN odor responses depend on the nonlinear integration of a complex set of inputs, which include feedforward excitation from ORNs, lateral excitation from cholinergic local neurons (eLNs) and lateral inhibition from GABAergic local neurons (iLNs)[42]. In the antennal lobe, the strength of each of these inputs is stereotypical in each glomerulus[41,49,54,57]. PN plasticity could theoretically arise from changes in any of these inputs, as well as changes in the intrinsic biophysical properties of the PN that impact signal integration. The observation that chronic focal activation of ORN input to a single glomerulus can elicit changes in odor coding in PNs belonging to other glomeruli suggests that olfactory plasticity is not glomerulus-autonomous and, at a minimum, likely involves local lateral networks which mediate information flow across glomeruli. Indeed, past studies in insects have implicated local inhibitory networks in mediating short- and long-timescale plasticity in the antennal lobe. For instance, repeated encounters with a given odor over short time scales (seconds to minutes) restructures PN activity to increase the reliability of PN representations of the odor[71,72]; computational models indicate this plasticity can be explained by facilitation of inhibitory connections in the antennal lobe[73]. In plasticity elicited by odor experience on long timescales (days), past work suggests glomerulus-specific plasticity is mediated by the strengthening of inputs from specific genetically defined subsets of inhibitory LNs[6,8,32]. This mechanism assumes that patterns of activity in the neurites of inhibitory LNs, each of which ramify broadly in the vast majority of antennal lobe glomeruli, are selectively modified through an as-yet-undescribed process to regulate release sites in just one or a few glomeruli. Our observation that olfactory plasticity is not necessarily glomerulus-specific is consistent with the broadly innervating anatomical characteristics of both excitatory and inhibitory LNs.

Prior work in fly found that chronic exposure to esters increased the sensitivity of ORNs to these odors[45,46], and multiple studies in rodents have concluded that chronic odor exposure evokes plasticity in ORN responses[58,74–78]. We considered the possibility that large changes in ORN sensitivity were not reflected in PN odor responses due to compensatory adjustments in

other parts of the antennal lobe circuitry. Direct measurements of how chronic odor exposure impacted ORN odor coding, PN intrinsic properties, ORN-PN synaptic strength, and lateral excitation revealed that, overall, most circuit properties were remarkably stable to a major perturbation in the flies' olfactory environment. For instance, the olfactory responses of ORNs in multiple glomeruli, as measured by single sensillum extracellular recordings and by population calcium imaging, were unaffected by strong, chronic excitation and were stable across a wide range of odor concentrations. Likewise, PN intrinsic properties and ORN-PN synaptic strength were similarly invariant to chronic odor exposure. However, we found that the strength of lateral excitatory coupling among glomeruli was increased in flies chronically exposed to the odor E2-hexenal. This result suggests a possible mechanism for the overall increased excitability of PNs in E2-hexenal exposed flies, particularly in the weak stimulus regime in which lateral excitation has the most impact[57]. Changes in the strength of lateral excitatory coupling between eLNs and PNs have been previously implicated in the slow recovery of odor responses in PNs that have chronically lost afferent ORN input due to injury[79]. Thus, the lateral excitatory network might serve as a common substrate for olfactory plasticity in multiple contexts.

Implications for understanding odor experience-dependent changes in olfactory behavior

Many studies in insect and in mammals have demonstrated that prior experience with an odor impacts how an animal subsequently responds to it. Establishing the directionality of olfactory plasticity – whether olfactory PNs respond less, more, or no differently to overrepresented odors in the environment – is important for understanding olfactory behavioral plasticity. Reports of reduced PN responses to overrepresented odors in the environment[6,8] were central to the interpretation of reduced behavioral aversion of flies towards familiar odors as a form of behavioral habituation. However, since nearly all studies use high concentrations of monomolecular odor (from a ~1-20% v/v source), which are nearly always aversive to animals,

these experiments do not disambiguate whether reduced behavioral aversion reflects behavioral habituation to an aversive odor or increased attraction (or tolerance) to an aversive odor. In one study where flies were chronically exposed to monomolecular odors at lower concentrations (~0.01% to 1%) that are attractive to flies, odor experience increased behavioral attraction towards the familiar odor[45]. In agreement, other work from our laboratory shows that chronic exposure of flies in early life to odors from natural sources increases behavioral attraction to these odors (in review[80]). These observations argue against habituation being the dominant effect of chronic odor exposure on behavior, since, if that were the case, reduced attraction to familiar attractive odors is expected.

Prior studies have suggested that experience-dependent modification of olfactory behavior in fly stems from odor-specific changes in the structure and function of the antennal lobe, which act to reduce PN sensitivity to frequent or abundant odors in the environment [6,8,35,40]. The overall stability of odor coding in PNs, the major output from the antennal lobe, in the face of significant perturbations in the odor environment that chronically alter the distribution of sensory input to the fly olfactory system, argue against this idea. Indeed, given that most typical odors are broadly encoded across many glomeruli, glomerulus-selective plasticity in the antennal lobe would seem to be an inefficient substrate for odor-specific plasticity since most individual glomeruli participate in the representation of many different odors.

If chronic exposure to odors in early life is reinterpreted as an increase in attraction or acceptance of familiar odors, rather than habituation towards them, our observation of stable PN responses in odor-exposed flies suggests that the neural mechanism responsible for behavioral plasticity likely acts downstream of the antennal lobe. One higher order olfactory area which receives antennal lobe output, the mushroom body, has been extensively studied for its role in associative learning[81]. Indeed, chronic odor exposure experiments are nearly always, by necessity, carried out in the presence of food, which may signal to flies a positive value of the

environment and become associated with the odor. More work is needed to evaluate how behavioral plasticity elicited by chronic odor exposure may depend on additional features of the environment, for instance, if exposure occurs in a passive versus rewarding (or aversive) context.

Implications for general principles of sensory plasticity

The stability of odor responses in early olfactory processing areas, even when challenged with persistent perturbations in the sensory environment, may reflect a more general design principle of sensory circuits. Even in mammalian nervous systems, which exhibit an overall higher degree of neural plasticity than insect systems, the function of early stages of sensory processing closer to the periphery is less dependent on normal sensory experience than later stages of cortical processing. For example, although normal visual experience is required for normal topographic maps, orientation selectivity, and direction selectivity in higher visual areas[1,82,83], the structure and function of retinal circuitry is much less impacted by abnormal visual experience[84,85]. Taking the case of direction selectivity as an example, whereas raising animals in the dark prevents the emergence of direction-selective responses in primary visual cortex[86,87], direction-selective ganglion cells in the retina have mature responses at birth, and they have normal directional tuning, speed tuning, and anatomy in dark-reared animals[85,88,89]. Thus, in both insects and vertebrates, experience-independent processes, specified by developmental genetic programs, appear to dominate in determining the structure and function of early stages of sensory processing, with the role of sensory experience becoming more prominent in higher-order stages of processing.

Why might plasticity be limited in early stages of sensory processing? Neural plasticity, like any form of phenotypic plasticity, comes at a cost. For instance, plasticity at the sensory periphery could be subject to an information acquisition cost, stemming from poor reliability or undersampling of the stimuli being used to evaluate the statistical structure of the environment.

Unreliable information about the environment could result in potentially even more inefficient sensory coding. Another potential cost of plasticity could arise from temporal mismatching, for instance, if the stimulus structure of the environment were to shift more rapidly than the time scale over which neural plasticity could be implemented. Generating a stable representation of the world at early stages of processing, which is invariant to local shifts in the stimulus environment, may be the best strategy. The initial sensory representation is relayed to multiple higher order processing areas, each of which may use the sensory information for different behavioral tasks. Neural plasticity acting at later stages of processing may allow different downstream circuits to independently reformat the sensory representation in a way that best subserves its specialized function.

SUPPLEMENTARY MATERIALS

Supplemental Table 1: Complete genotypes and *n* for all experiments.
Solvent is paraffin oil.

FIGURE	GENOTYPE	EXPERIMENTAL GROUP	STIMULUS	NO. FLIES (*N*)
1C-D	*NP3481-Gal4, UAS-CD8:GFP* (X)	E2-hexenal	solvent	1
			E2-hexenal, 10^{-7}	1
2**B-F** 2Q	*NP3481-Gal4, UAS-CD8:GFP* (X)	E2-hexenal exposed	solvent	3
			E2-hexenal, 10^{-12}	3
			E2-hexenal, 10^{-11}	5
			E2-hexenal, 10^{-10}	**9**
			E2-hexenal, 10^{-9}	**10**
			E2-hexenal, 10^{-8}	**11**
			E2-hexenal, 10^{-7}	**12**
			E2-hexenal, 10^{-6}	10
			E2-hexenal, 10^{-5}	6
		solvent exposed	solvent	3
			E2-hexenal, 10^{-12}	3
			E2-hexenal, 10^{-11}	3
			E2-hexenal, 10^{-10}	**8**
			E2-hexenal, 10^{-9}	**7**
			E2-hexenal, 10^{-8}	**19**
			E2-hexenal, 10^{-7}	**19**

			E2-hexenal, 10^{-6}	14
			E2-hexenal, 10^{-5}	9
2**H-J** 2R **3F**	*NP3481-Gal4, UAS-CD8:GFP* (X)	2-butanone exposed	2-butanone, 10^{-8}	4
			2-butanone, 10^{-7}	**11**
			2-butanone, 10^{-6}	**12**
			2-butanone, 10^{-5}	**13**
			2-butanone, 10^{-4}	**12**
		solvent exposed	2-butanone, 10^{-8}	6
			2-butanone, 10^{-7}	**16**
			2-butanone, 10^{-6}	**13**
			2-butanone, 10^{-5}	**14**
			2-butanone, 10^{-4}	**11**
2L-P 2S	*UAS-CD8:GFP* (X)*; MZ612-Gal4, UAS-CD8:GFP* (II)	geranyl acetate exposed	geranyl acetate, 10^{-7}	7
			geranyl acetate, 10^{-6}	9
			geranyl acetate, 10^{-5}	9
			geranyl acetate, 10^{-4}	8
		solvent exposed	geranyl acetate, 10^{-7}	10
			geranyl acetate, 10^{-6}	11
			geranyl acetate, 10^{-5}	11
			geranyl acetate, 10^{-4}	8
3B-E 3G-H	*NP3481-Gal4, UAS-CD8:GFP* (X)	E2-hexenal exposed	2-butanone, 10^{-7}	6
			2-butanone, 10^{-6}	8
			2-butanone, 10^{-5}	7
			2-butanone, 10^{-4}	5
		solvent exposed	2-butanone, 10^{-7}	16
			2-butanone, 10^{-6}	13
			2-butanone, 10^{-5}	14
			2-butanone, 10^{-4}	11
3J-N	*UAS-CD8:GFP* (X)*; MZ612-Gal4, UAS-CD8:GFP* (II)	E2-hexenal exposed	geranyl acetate, 10^{-7}	5
			geranyl acetate, 10^{-6}	5
			geranyl acetate, 10^{-5}	5
			geranyl acetate, 10^{-4}	5
		solvent exposed	geranyl acetate, 10^{-7}	10
			geranyl acetate, 10^{-6}	11
			geranyl acetate, 10^{-5}	11
			geranyl acetate, 10^{-4}	8
4B-F	*UAS-CD8:GFP* (X)*; MZ612-Gal4, UAS-CD8:GFP* (II)	20% geranyl acetate exposed	geranyl acetate, 10^{-7}	5
			geranyl acetate, 10^{-6}	5
			geranyl acetate, 10^{-5}	5
			geranyl acetate, 10^{-4}	6
		solvent exposed	geranyl acetate, 10^{-7}	5
			geranyl acetate, 10^{-6}	5
			geranyl acetate, 10^{-5}	5
			geranyl acetate, 10^{-4}	6

4H-L	*NP3481-Gal4, UAS-CD8:GFP* (X)	20% geranyl acetate exposed	valeric acid, $5x10^{-4}$	6
			valeric acid, 10^{-3}	6
			valeric acid, $5x10^{-3}$	6
			valeric acid, 10^{-2}	6
		solvent exposed	valeric acid, $5x10^{-4}$	6
			valeric acid, 10^{-3}	6
			valeric acid, $5x10^{-3}$	6
			valeric acid, 10^{-2}	5
5B-C	*NP3481-Gal4, UAS-CD8:GFP* (X)	2-butanone exposed	*pentyl acetate, 10^{-3}*	
			+2-butanone, 10^{-8}	3
			+2-butanone, 10^{-7}	7
			+2-butanone, 10^{-6}	6
			+2-butanone, 10^{-5}	7
			+2-butanone, 10^{-4}	6
		solvent exposed	*pentyl acetate, 10^{-3}*	
			+2-butanone, 10^{-8}	6
			+2-butanone, 10^{-7}	6
			+2-butanone, 10^{-6}	6
			+2-butanone, 10^{-5}	7
			+2-butanone, 10^{-4}	5
5E-F	*NP3481-Gal4, UAS-CD8:GFP* (X)	E2-hexenal exposed	*pentyl acetate, 10^{-3}*	
			+2-butanone, 10^{-8}	3
			+2-butanone, 10^{-7}	3
			+2-butanone, 10^{-6}	4
			+2-butanone, 10^{-5}	3
			+2-butanone, 10^{-4}	3
		solvent exposed	*pentyl acetate, 10^{-3}*	
			+2-butanone, 10^{-8}	6
			+2-butanone, 10^{-7}	6
			+2-butanone, 10^{-6}	6
			+2-butanone, 10^{-5}	7
			+2-butanone, 10^{-4}	5
S5A	*+/UAS-brp.S-mStraw* (II)*; 20XUAS-CD8:GFP/NP3056-Gal4* (III)	solvent exposed	NA	1
S5B S5D S5F S5H	*+/UAS-brp.S-mStraw* (II)*; 20XUAS-CD8:GFP/NP3056-Gal4* (III)	2-butanone exposed	NA	13
		solvent exposed	NA	10
S5C S5E S5G S5I	*+/UAS-brp.S-mStraw* (II)*; 20XUAS-CD8:GFP/NP3056-Gal4* (III)	E2-hexenal exposed	NA	11
		solvent exposed	NA	8

6B 6C	*NP3481-Gal4, UAS-CD8:GFP* (X)	E2-hexenal exposed	solvent	12
			E2-hexenal, 10^{-12}	11
			E2-hexenal, 10^{-11}	11
			E2-hexenal, 10^{-10}	10
			E2-hexenal, 10^{-9}	10
			E2-hexenal, 10^{-8}	8
			E2-hexenal, 10^{-7}	9
			E2-hexenal, 10^{-6}	9
			E2-hexenal, 10^{-5}	9
			E2-hexenal, 10^{-4}	10
		solvent exposed	solvent	9
			E2-hexenal, 10^{-12}	9
			E2-hexenal, 10^{-11}	9
			E2-hexenal, 10^{-10}	8
			E2-hexenal, 10^{-9}	8
			E2-hexenal, 10^{-8}	9
			E2-hexenal, 10^{-7}	9
			E2-hexenal, 10^{-6}	7
			E2-hexenal, 10^{-5}	6
			E2-hexenal, 10^{-4}	6
6E 6F	*NP3481-Gal4, UAS-CD8:GFP* (X)	2-butanone exposed	solvent	6
			2-butanone, 10^{-10}	9
			2-butanone, 10^{-9}	9
			2-butanone, 10^{-8}	9
			2-butanone, 10^{-7}	10
			2-butanone, 10^{-6}	10
			2-butanone, 10^{-5}	9
			2-butanone, 10^{-4}	10
			2-butanone, 10^{-3}	9
		solvent exposed	solvent	9
			2-butanone, 10^{-10}	11
			2-butanone, 10^{-9}	10
			2-butanone, 10^{-8}	10
			2-butanone, 10^{-7}	10
			2-butanone, 10^{-6}	9
			2-butanone, 10^{-5}	9
			2-butanone, 10^{-4}	9
			2-butanone, 10^{-3}	9
6H 6I	*NP3481-Gal4, UAS-CD8:GFP* (X)	E2-hexenal exposed	solvent	5
			2-butanone, 10^{-10}	9
			2-butanone, 10^{-9}	9
			2-butanone, 10^{-8}	9
			2-butanone, 10^{-7}	9
			2-butanone, 10^{-6}	9

			2-butanone, 10^{-5}	8
			2-butanone, 10^{-4}	8
			2-butanone, 10^{-3}	9
		solvent exposed	solvent	9
			2-butanone, 10^{-10}	11
			2-butanone, 10^{-9}	10
			2-butanone, 10^{-8}	10
			2-butanone, 10^{-7}	10
			2-butanone, 10^{-6}	9
			2-butanone, 10^{-5}	9
			2-butanone, 10^{-4}	9
			2-butanone, 10^{-3}	9
6K	*+/Or7a-Gal4*(KI) (X)*; +/20XUAS-IVS-syn21-opGCaMP6f-p10* (II)	solvent exposed	E2-hexenal, 10^{-7}	1
6L 6M	*+/Or7a-Gal4*(KI) (X)*; +/20XUAS-IVS-syn21-opGCaMP6f-p10* (II)	E2-hexenal exposed	solvent	8
			E2-hexenal, 10^{-12}	6
			E2-hexenal, 10^{-11}	8
			E2-hexenal, 10^{-10}	8
			E2-hexenal, 10^{-9}	8
			E2-hexenal, 10^{-8}	8
			E2-hexenal, 10^{-7}	7
			E2-hexenal, 10^{-6}	8
		solvent exposed	solvent	8
			E2-hexenal, 10^{-12}	6
			E2-hexenal, 10^{-11}	8
			E2-hexenal, 10^{-10}	8
			E2-hexenal, 10^{-9}	8
			E2-hexenal, 10^{-8}	8
			E2-hexenal, 10^{-7}	7
			E2-hexenal, 10^{-6}	8
7B-C	*NP3481-Gal4, UAS-CD8:GFP* (X)	E2-hexenal exposed	NA	4
		solvent exposed	NA	4
7E	*NP3481-Gal4, UAS-CD8:GFP* (X)*; +/13xlexAop2-IVS-CsChrimson.mVenus* (II)*; +/Or7a-lexA* (III)	solvent exposed	NA	1
7F-G	*NP3481-Gal4, UAS-CD8:GFP* (X)*; +/13xlexAop2-IVS-CsChrimson.mVenus* (II)*; +/Or7a-lexA* (III)	E2-hexenal exposed	NA	5
		solvent exposed	NA	7
7I-J	*UAS-CD8:GFP* (X)*; MZ612-Gal4, UAS-CD8:GFP* (II)	E2-hexenal exposed	solvent	3
			pentyl acetate	3
			2-heptanone	3

			E2-hexenal	3
			isobutyl acetate	3
			p-cresol	3
			2-butanone	3
		solvent exposed	solvent	3
			pentyl acetate	5
			2-heptanone	4
			E2-hexenal	4
			isobutyl acetate	4
			p-cresol	4
			2-butanone	3

661

662

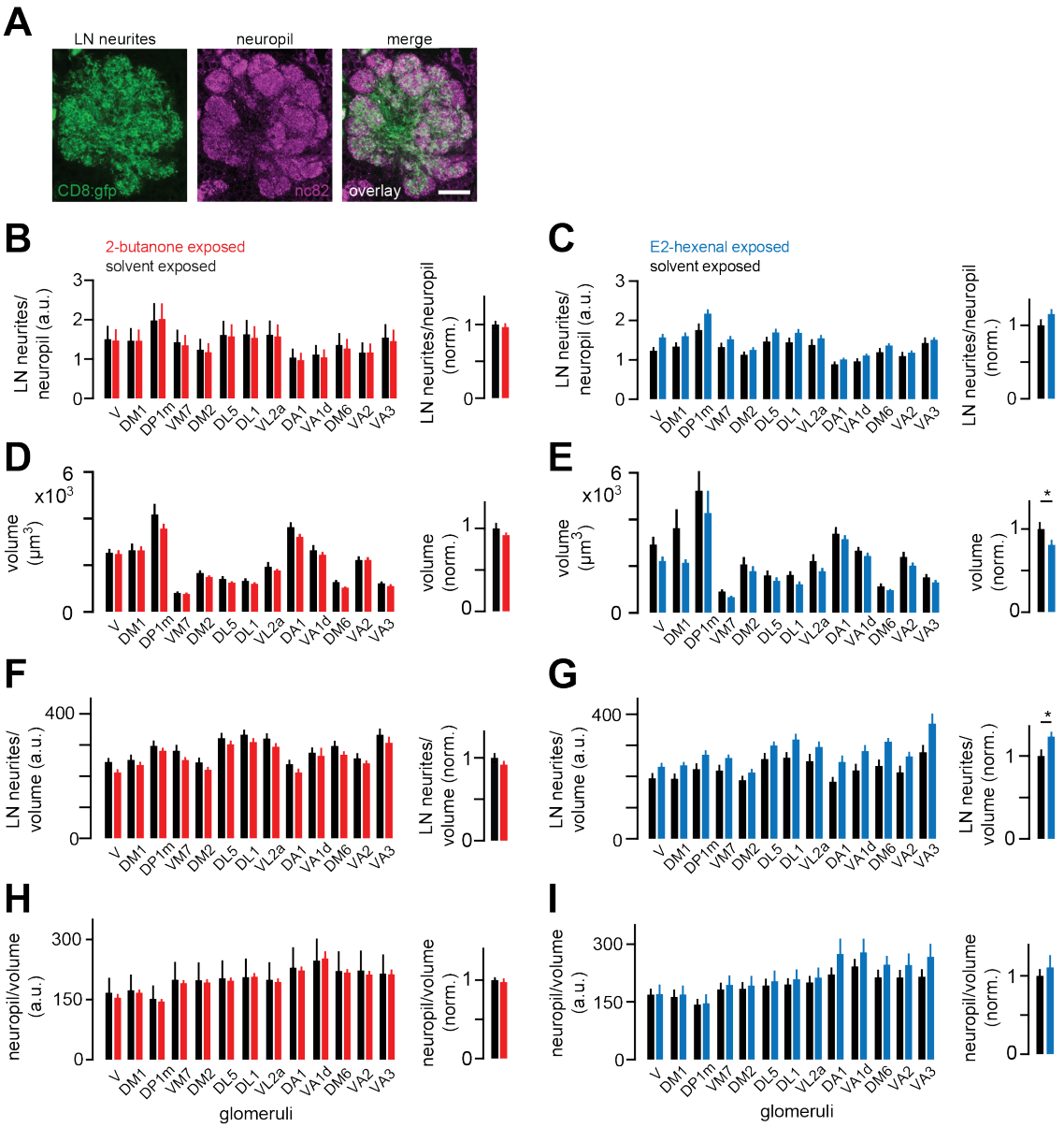

Figure 5 – figure supplement 1: LN innervation of antennal lobe glomeruli is unchanged by chronic excitation of a single ORN class.

A) Single confocal section through the antennal lobe of a fly expressing membrane-targeted GFP (CD8:GFP, green) in a large subset of LNs. Synaptic neuropil was immunostained using the nc82 antibody (magenta) to visualize glomerular boundaries. Scale bar, 20µm.

B-C) *Left:* Ratios of mean LN neurite signal to mean synaptic neuropil signal in each indicated glomerulus in flies chronically exposed to solvent (paraffin oil) versus 2-butanone (10^{-4}) **(B)**, or to solvent (paraffin oil) versus E2-hexenal (10^{-7}) **(C)**. *Right:* Mean normalized ratio of LN neurites to neuropil across glomeruli. Within each glomerulus, values were normalized to the mean ratio of the solvent-exposed group.

D-E) Same as **B-C)** but for the volume of each glomerulus.

F-G) Same as **B-C)** but for the volumetric density of LN neurite signal in each glomerulus.

H-I) Same as **B-C)** but for the volumetric density of synaptic neuropil signal in each glomerulus.

All plots are mean ± SEM across flies in each experimental condition, n=8-13 flies. *p<0.05, two-tailed Mann-Whitney U-test with Bonferroni multiple comparisons adjustment. See Supplemental Table 1 for the full genotype and number of flies in every condition.

Figure 5 – source data 2

Source data for Figure 5B-I.

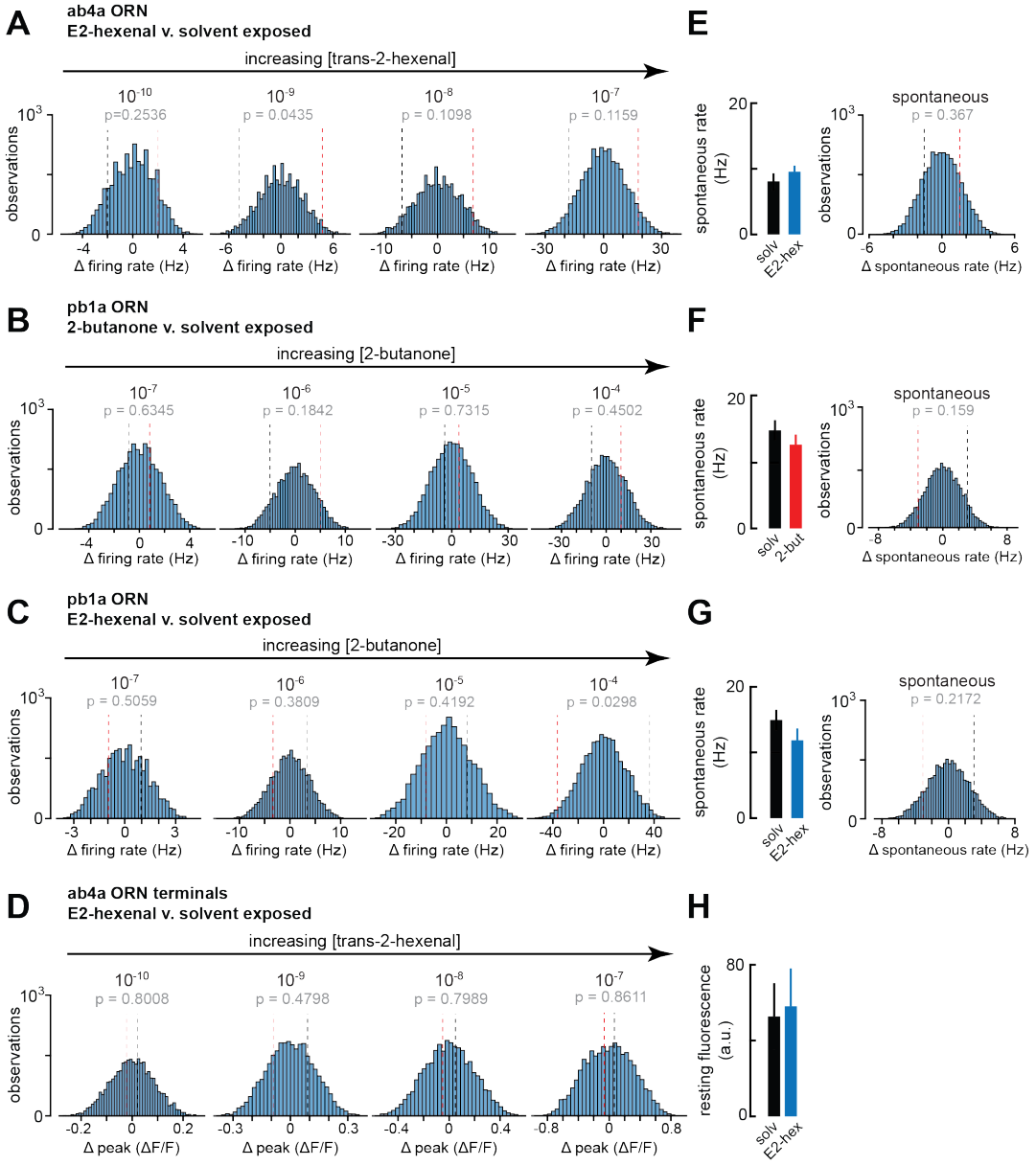

Figure 6 – figure supplement 1: Statistical analysis of spontaneous and odor-evoked ORN firing rates in odor- and solvent-exposed flies.

A-D) Histograms of the difference between group means in 10,000 permutations of the datasets for each indicated comparison of odor-evoked firing rates in **A)** ab4a ORNs from E2-hexenal- or solvent-exposed flies (from **Figure 6B**); **B)** pb1a ORNs from 2-butanone- or solvent-exposed flies (from **Figure 6E**); **C)** pb1a ORNs from E2-hexenal- or solvent-exposed flies (from **Figure 6H**); and **D)** odor-evoked calcium signals from ab4a ORN axon terminals in E2-hexenal- or solvent-exposed flies (from **Figure 6L**). The p-value for each comparison is computed as the fraction of absolute resampled differences larger than the absolute observed difference (e.g., the fraction of the distribution lying outside the dotted bounds).

E-G) Mean spontaneous firing rate, and statistical comparison of means, computed over a 5 s window prior to stimulus onset in ORNs corresponding to each condition in **A-C)**.

H) Mean resting fluorescence computed over a 5 s window prior to stimulus onset in ab4a ORN terminals in the DL5 glomerulus in E2-hexenal- and solvent-exposed flies. None of the comparisons in **Figure 6** between odor- and solvent-exposed groups are statistically significant at the α=0.05 level (with Bonferroni adjustment for multiple comparisons).

Figure 7- figure supplement 1: PN intrinsic properties and latency of light-evoked EPSCs.
A) Membrane potential versus current for increasing steps of current injection (from **Figure 7B**) in deafferented DL5 PNs from E2-hexenal- and solvent-exposed flies.
B) Same as **A)** but plotting firing rate versus membrane potential at each current step.
C) EPSCs evoked by a 100 µs pulse of light (488 nm, ~0.175 mW/mm^2) in a deafferented DL5 PN from a solvent-reared fly expressing CsChrimson in presynaptic ab4a ORNs. Note the variable latency to the peak of the evoked EPSC, which is consistent with the approximate latency of the first light-evoked spike in ORN recordings from in the antenna. EPSCs are aligned by their peaks for averaging across trials in **Figure 7E-G**.

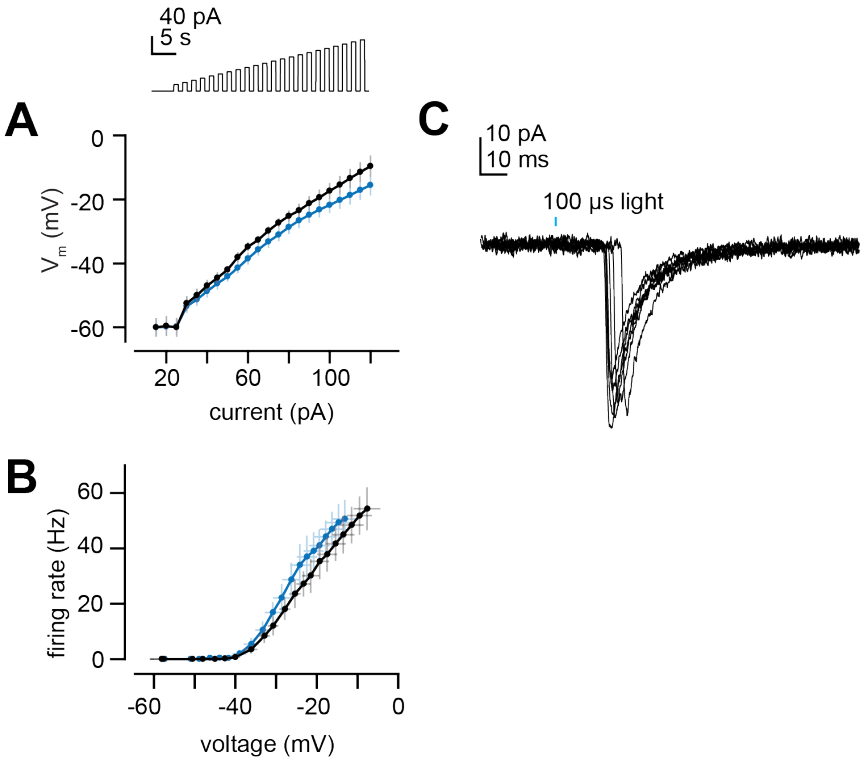

663

664

665

METHODS

Flies

Drosophila melanogaster were raised on a 12:12 light:dark cycle at 25°C and 70% relative humidity on cornmeal/molasses food containing: water (17.8 l), agar (136 g), cornmeal (1335.4 g), yeast (540 g), sucrose (320 g), molasses (1.64 l), $CaCl_2$ (12.5 g), sodium tartrate (150 g), tegosept (18.45 g), 95% ethanol (153.3 ml) and propionic acid (91.5 ml). All experiments were performed in 2-day old female flies. The specific genotype of the flies used in each experiment are given in Supplemental Table 1. The transgenes used in this study were acquired from the Bloomington Drosophila Stock Center (BDSC) or the Kyoto Drosophila Stock Center (DGGR), unless otherwise indicated. They have been previously characterized as follows: *NP3481-Gal4* (Kyoto:113297) labels DL5, VM7, and DM6 PNs[54,90]; *MZ612-Gal4* (II) (gift of L. Luo) labels VA6 PNs[91]; *Or7a-Gal4*(KI) (gift of C. Potter) expresses Gal4 from the *Or7a* locus under the control of its endogenous regulatory elements[92]; *UAS-CD8:GFP* (X) (RRID:BDSC_5136) and *UAS-CD8:GFP* (II) (RRID:BDSC_5137) express CD8-tagged GFP, which is targeted to the membrane, under Gal4 control[93]; *20xUAS-IVS-CD8:GFP* (attP2) (RRID:BDSC_32194) expressed CD8-tagged GFP under Gal4 control[94]*; UAS-brp.S-mStrawberry* (II) (gift of S. Sigrist) expresses a red fluorescent protein-tagged short-form of bruchpilot[95]; *20xUAS-IVS-syn21-opGCaMP6f-p10* (su(Hw)attP5) (gift of B. Pfeiffer and D. Anderson) expresses codon-optimized GCaMP6f under Gal4 control[96]; and *13xlexAop2-IVS-CsChrimson.mVenus* (attP40) (RRID:BDSC_55138) expresses a Venus-tagged red-shifted channelrhodopsin CsChrimson under lexA control[52].

Or7a-lexA (III) flies were generated as follows. The *Or7a* promoter was PCR amplified from a bacterial artificial chromosome (RPCI-98 library, clone 39F18, BACPAC Resources) containing the *or7a* locus of *D. melanogaster* using primers 5'-ACCGCATCCCGATCAAGACACAC-3' and

690 5'-TGATGGACTTTTGACGCCTGGGAATA-3'. The *Or7a* promoter was inserted 5' to *nlslexA::p65*
691 using isothermal assembly in vector *pBPnlslexA::p65Uw*, replacing the ccdB cassette. The
692 plasmid *pBPnlslexA::p65Uw* was a gift from G. Rubin (Addgene plasmid #26230,
693 RRID:Addgene_26230). The final sequence of the construct was confirmed by Sanger
694 sequencing, and transgenic flies were generated by site-specific integration into the VK00027
695 landing site (BestGene, Inc., Chino Hills, CA). To verify the selectivity of the driver, *Or7a-lexA* was
696 crossed to *13xlexAop2-mCD8:GFP* (RRID:BDSC_32205), and brains of the resulting progeny
697 flies (2 days old) were dissected and immunostained with antibodies against GFP and nc82.
698 GFP expression was observed selectively in ab4a ORN axons projecting to the DL5 glomerulus;
699 no other signal was observed in the central brain.
700
701 **Chronic odor exposure**
702 With the exception of Figure 4, all data were from flies were chronically exposed to solvent or
703 specific monomolecular odors while reared in standard fly bottles containing cornmeal/molasses
704 food and sealed with modified cotton plugs through which two thin-walled stainless-steel hollow
705 rods (~5 cm length, ~3.2 mm inner diameter) were tightly inserted, serving as an inlet and an
706 outlet for air flow. The bottom of the cotton plug was lined with mesh (McMaster-Carr #9318T45)
707 to prevent flies from entering the rods. The inlet port was fit with a luer connector for easy
708 connection to the carrier stream; the outlet port was vented with loose vacuum suction.
709 The odor environment inside the bottle was controlled by delivering to the inlet of the
710 bottle a stream of charcoal-filtered, humidified air (275 ml/min), with a small fraction of the air
711 stream (odor stream, 25 ml/min) diverted into the headspace of a control vial filled with solvent
712 (paraffin oil, J.T. Baker, VWR #JTS894-7) before it was reunited with the carrier stream (250
713 ml/min). Air flow rates were controlled using variable area valved flow meters (Cole-Parmer). In
714 response to an external 5V command, a three-way solenoid valve redirected the 25 ml/min odor

715 stream from the headspace of the control solvent vial through the headspace of the vial
716 containing diluted odor for 1 second. The diluted odor was continuously stirred using a miniature
717 magnetic stir bar and stir plate (homebrewing.org). Delivery of the 1-second pulse of odor into
718 the carrier stream was repeated every 21 seconds. Tygon tubing (E-3603) was used throughout
719 the odor delivery system, with the exception of a portion of the carrier stream where odor entered
720 and the path from the odor vial to the input to the carrier stream, where PTFE tubing was used.
721 The stability of the amplitude of the odor pulse over the course of 24 hours was measured
722 using a photoionization detector (200B miniPID, Aurora Instruments), with the sensor probe
723 mounted at the center of a fresh fly bottle. Based on the observed rundown in the amplitude of
724 the odor pulse (Figure 1B), the odor vial in the odor delivery system was swapped out every 12
725 hours for a fresh dilution of odor during chronic exposure experiment with flies. Under these
726 conditions, the amplitude of the odor pulse was not expected to decrease more than ~20% at
727 any point during the exposure period.
728 Flies were seeded in a fresh fly bottle at low density (~7-8 females). The evening prior to
729 expected eclosion, any adult flies were removed from the bottle, and controlled odor delivery
730 was initiated into the bottle. The next morning (day 0), newly eclosed flies were transferred into
731 a fresh bottle and controlled odor delivery was continued for another ~48 hours. Experiments
732 were typically conducted on day 2, with the exception of those in Figure 4.
733 In Figure 4, flies were chronically exposed to a sustained high concentration of
734 monomolecular odor from a stationary source placed in the bottle[6,35]. The evening prior to
735 eclosion, growth bottles were cleared of any adult animals, and a 2-ml glass vial containing 1
736 mL of geranyl acetate (20% v/v) was placed into the bottle. The vial opening was covered with a
737 layer of porous mesh, held securely in place with a silicone o-ring fitted around the mouth of the
738 vial. The growth bottle was sealed with a standard cotton plug with no inlets/outlets. The next
739 morning, newly eclosed flies were transferred into a fresh bottle containing a fresh odor source,

and, thereafter, the odor source was renewed daily until day 5, when experiments were conducted.

Odor concentrations in this study are referred to by the v/v dilution factor of the odor in paraffin oil in the odor vial. For chronic odor exposure in Figures 1-3 and 5-7, flies were exposed to odors at dilution factors of 10^{-7} for E2-hexenal, 10^{-4} for 2-butanone, and 10^{-4} for geranyl acetate. Headspace concentrations were further diluted 1:11 in air prior to delivery to the fly bottle. Flies were chronically exposed to pulses of odor (in gas phase) that are estimated from published vapor pressure data at 25ºC[97] to be ~1 ppb for E2-hexenal (10^{-7}), ~13000 ppb for 2-butanone (10^{-4}), and ~4 ppb for geranyl acetate (10^{-4}). For chronic odor exposure in Figure 4, flies were exposed to geranyl acetate at a dilution factor of 0.2 corresponding to ~7900 ppb in air.

The mean spontaneous firing rates of the PNs (DL5, VM7, VA6) investigated in this study range from ~3-7 Hz, and each 1-sec odor pulse delivered during chronic odor exposure elicits ~150 spikes in PNs (Figure 1). Thus, chronic odor exposure approximately doubles overall PN firing rates (from ~180-420 spikes/min to 690-930 spikes/min) and elicits ~1.3 million extra spikes in a specific PN type over the course of two days.

Electrophysiological recordings

PN recordings

Electrophysiological measurements were performed on 2 day-old female flies essentially as previously described[98], except in Figure 4, where recordings were established from 5 day-old female flies. The rate of establishing successful recordings was significantly lower in Figure 4, approximately 1 in 5 attempts compared to the usual rate of approximately 1 in 2 attempts. Flies were briefly cold-anesthetized and immobilized using wax. The composition of the internal pipette solution for current clamp recordings in PNs was (in mM): potassium aspartate 140, HEPES 10, MgATP 4, Na_3GFP 0.5, EGTA 1, KCl 1, biocytin hydrazide 13. The internal solution

765 was adjusted to a pH of 7.3 with KOH or aspartic acid and an osmolarity between 262-268
766 mOsm. For voltage-clamp recordings, an equal concentration of cesium was substituted for
767 potassium. The external solution was Drosophila saline containing (in mM): NaCl 103, KCl 3, N-
768 tris(hydroxymethyl) methyl-2-aminoethane-sulfonic acid 5, trehalose 8, glucose 10, $NaHCO_3$ 26,
769 NaH_2PO_4 1, $CaCl_2$ 1.5, $MgCl_2$ 4. The pH of the external solution was adjusted to 7.2 with HCl or
770 NaOH (when bubbled with 95% O_2/5% CO_2), and the osmolarity was adjusted to ~270-275
771 mOsm. Recording pipettes were fabricated from borosilicate glass and had a resistance of ~6-
772 8 MΩ. Recordings were acquired with a MultiClamp 700B (Axon Instruments) using a CV-7B
773 headstage (500 MΩ). Data were low-pass filtered at 5 kHz, digitized at 10 kHz, and acquired in
774 MATLAB (Mathworks, Natick, MA). Voltages are uncorrected for liquid junction potential.
775 Flies were removed from the odor exposure environment at least one hour prior to
776 recordings, briefly cold-anesthetized anesthetized, and recordings were performed at room
777 temperature. Recordings with respect to experimental groups (odor-exposed versus solvent-
778 exposed) were conducted in a quasi-randomized order; the experimenter was not masked to
779 experimental condition. PN somata were visualized with side illumination form an infrared LED
780 (Smartvision) under a 40x water immersion objective on an upright compound microscope
781 equipped with an epifluorescence module and 488 nm blue light source (Sutter Lambda TLED+).
782 Whole-cell patch-clamp recordings were targeted to specific PNs types based on GFP
783 fluorescence directed by genetic drivers. Three PN types were targeted in this study: DL5 and
784 VM7 using *NP3481-Gal4* and VA6 using *MZ612-Gal4*. One neuron was recorded per brain. PN
785 identity was confirmed using diagnostic odors, and the morphology (and thus identity) of all PNs
786 was further verified posthoc by streptavidin staining in fixed brains. Cells with little or no
787 spontaneous activity upon break-in, suggesting antennal nerve damage, were discarded. Input
788 resistance was monitored on every trial in real-time, and recordings were terminated if the input
789 resistance of the cell drifted by more than 20%.

For experiments in Figure 7, the antennal nerves were bilaterally severed immediately prior to recordings using fine forceps.

ORN recordings

Single-sensillum recordings were performed essentially as previously described[99]. Flies were removed from the odor exposure environment at least one hour prior to recordings, briefly cold-anesthetized, and recordings were performed at room temperature. Briefly, flies were immobilized in the end of a trimmed pipette tip using wax, and one antenna or one palp was visualized under a 50x air objective. The antenna was stabilized by tightly sandwiching it between a set of two fine glass hooks, fashioned by gently heating pipettes pulled from glass capillaries (World Precision Instruments, TW150F-3). The palp was stabilized from above with a fine glass pipette pressing it firmly against a glass coverslip provided from below. A reference electrode filled with external saline (see above) was inserted into the eye, and a sharp saline-filled glass recording microelectrode was inserted into the base of the selected sensillum under visual control. Recordings from ab4 and pb1 sensilla were established in the antenna and palp, respectively, based on the characteristic size and morphology of the sensillum, its position on the antenna, and the presence of two distinct spike waveforms, each having a characteristic odor sensitivity and spontaneous firing frequency[21]. Signals were acquired with a MultiClamp 700B amplifier, low-pass filtered at 2 kHz, digitized at 10 kHz, and acquired in MATLAB. Single-sensillum recordings were performed in 2-day old *NP3481-Gal4, UAS-CD8:GFP* females to allow direct comparisons to PN data.

Odor stimuli

Odors used in this study were benzaldehyde, 2-butanone, *p*-cresol, geosmin, geranyl acetate, 2-heptanone, E2-hexenal, isobutyl acetate, and pentyl acetate. All odors were obtained from

MilliporeSigma or Fisher Scientific at the highest purity available (typically >99%). Odor stimuli are referred to by their v/v dilution factor in paraffin oil. Each 20-ml odor vial contained 2 ml of diluted odor in paraffin oil. Diagnostic stimuli that distinguished targeted PN types from other labeled PN types in the driver line used were as follows: for DL5 PNs, E2-hexenal (10^{-8}) and benzaldehyde (10^{-4}); for VM7 PNs, 2-butanone (10^{-7}) and isobutyl acetate (10^{-4}); and for VA6 PNs, geranyl acetate (10^{-6}). Diagnostic stimuli for ORN classes were as follows: for the ab4 sensillum on the antenna, E2-hexenal (10^{-7}) for the ab4a "A" spike and geosmin (10^{-2}) for the ab4b "B" spike; and for the pb1 sensillum on the palp, 2-butanone (10^{-5}) for the pb1a "A" spike and *p*-cresol (10^{-3}) for the pb1b "B" spike.

Fresh odor dilutions were made every 5 days. Each measurement in a fly represents the mean of 5 trials for ORN responses or 6 trials for PN responses, spaced 40 seconds apart. Solvent (paraffin oil) trials were routinely interleaved to assess for contamination. Stimuli were presented in pseudo-randomized order, except for measurements of concentration-response curves where odors were presented from low to high concentrations.

Odors were presented during recordings from olfactory neurons essentially as previously described[99]. In brief, a constant stream of charcoal-filtered air (2.22 L/min) was directed at the fly, with a small portion of the stream (220 mL/min) passing through the headspace of a control vial filled with paraffin oil (solvent) prior to joining the carrier stream (2.0 L/min). Air flow was controlled using mass flow controllers (Alicat Scientific). When triggered by an external voltage command, a three-way solenoid valve redirected the small portion of the stream (220 mL/min) from the solvent vial through the headspace of a vial containing odor for 500 ms; thus, the concentration of the odor in gas phase was further diluted ~10-fold prior to final delivery to the animal. The solvent vial and the odor vial entered the carrier stream at the same point, ~10 cm from the end of the tube. The tube opening measured ~4 mm in diameter and was positioned ~1 cm away from the fly. We presented 500-ms pulses of odor unless otherwise indicated.

Odor mixtures (Figure 4) were generated by mixing in air. In these experiments, a second solenoid valve was added that diverted another small fraction of the carrier stream (220 ml/min) through either a second solvent vial or a second odor vial before rejoining the carrier stream. When the two solenoids were both triggered, they drew from the carrier stream at the same point, and the two odorized streams also both rejoined the carrier stream at about the same point, ~10 cm from the end of the delivery tube.

Immunohistochemistry

Intracellular biocytin fills were processed as previously described[98]. In brief, brains were fixed for 14 min at room temperature in freshly prepared 4% paraformaldehyde, incubated overnight in mouse nc82 primary antibody (1:40, Developmental Studies Hybridoma Bank #AB_2314866), then subsequently incubated overnight in Alexa Fluor 568 streptavidin conjugate (1:1000, Molecular Probes) and Alexa Fluor 633 goat anti-mouse (1:500, Molecular Probes). PN morphologies were reconstructed from serial confocal images through the brain at 40X magnification and 1-µm step size.

LN innervation was quantified in flies of genotype *+/UAS-brp.S-mStraw; 20XUAS-IVS-CD8:GFP/NP3056-Gal4*; the *brp.S-mStraw* signal was not measured. Immediately after dissection, brains were fixed for 14 min in freshly prepared 4% paraformaldehyde and incubated overnight in rat anti-CD8 (1:50, Thermo Fisher #MA5-17594) and mouse nc82 (1:40) primary antibodies, then subsequently incubated overnight in Alexa Fluor 488 goat anti-rat (1:500, Abcam #ab150157) and Alexa Fluor 633 goat anti-mouse (1:500, Thermo Fisher #A21050) secondary antibodies. All steps were performed at room temperature, and brains were mounted and imaged in Vectashield mounting medium (Vector labs). In pilot experiments, we compared direct GFP fluorescence in lightly fixed brain with amplified GFP signal using the standard protocol and observed weaker, but qualitatively similar signals. Confocal z-stacks at 1024x1024

resolution spanning the entire volume of the antennal lobe were collected on a Leica SP8 confocal microscope at 1 μm slice intervals using a 63× oil-immersion lens. Identical laser power and imaging settings were used for all experiments.

Calcium imaging

Calcium imaging of ab4a ORN terminals in the DL5 glomerulus was performed on 2-day old female flies essentially as previously described [41]. In brief, flies were cold-anesthetized and immobilized with wax. The antennal lobes were exposed by removal of the dorsal flap of head cuticle, and the brain was perfused with Drosophila saline (see above) that was cooled to 21°C (TC-324C, Warner Instruments) and circulated at a rate of 2-3 ml/min. GCaMP6f signals were measured on a two-photon microscope (Thorlabs, Sterling, VA) using a Ti-Sapphire femtosecond laser (MaiTai eHP DS, Spectra-Physics) at an excitation wavelength of 925 nm, steered by a galvo-galvo scanner. Images were acquired with a 20x water-immersion objective (XLUMPLFLN, Olympus) at 256x96 pixels, a frame rate of 11 Hz, and a dwell time of 2μs/pixel. The same laser power and imaging settings were maintained for all experiments. The microscope and data acquisition were controlled using ThorImage 3.0. The DL5 glomeruli were clearly labeled as bilateral spherical structures ~10 μm from the dorsal surface of the antennal lobes. In each trial, an 8 s period of baseline activity was collected immediately prior to stimulus presentation which was used to establish the level of baseline fluorescence of each pixel. Each odor stimulus was presented for 500 ms, for three trials, with a 45-s interstimulus interval.

Optogenetic stimulation of ORN axons

A stock solution of all-trans-retinal (Sigma-Aldrich, R2500) was prepared at 35 mM in 95% ethanol and stored at -20° C in the dark. The cross that generated the experimental flies was maintained in the dark. Newly eclosed experimental flies for optogenetic experiments were

transferred to standard cornmeal/molasses food supplemented with 350 μM all-trans-retinal mixed into the food and exposed to odor (or solvent) for two days in the dark.

After exposing the antennal lobes, the antennal nerves were acutely and bilaterally severed at their distal entry point into the first segment of the antennal, eliminating EPSCs derived from spontaneous ORN spiking. Electrophysiology rigs were light-proofed. Whole-cell recordings in voltage-clamp mode were established from DL5 PNs in flies expressing Chrimson in all ab4a ORNs (from *or7a-lexA*). DL5 PNs were identified based on GFP expression (from *NP3481-Gal4*) and the presence of light-evoked responses, and their identity was confirmed after the recording by processing the biocytin fill. In pilot experiments, we tested several methods for optical stimulation and were unable to achieve reliable stimulation of only a single ORN axon presynaptic to the recorded PN using excitation with 590 nm light from a fiber optic-coupled LED (Thorlabs M590F3 with Ø200 μm fiber, 0.22 NA). Excitation of ORN terminals was very sensitive to the position and angle of the optrode relative to the antennal nerve, and we found large variability in the amount of light (intensity and pulse duration) required to evoke EPSCs in the PN.

As an alternative approach, we used wide-field illumination from a 470-nm (blue) LED light source (Sutter Instrument, TLED+). We delivered light pulses of 100 μs duration at 30 s trial intervals, starting at very low levels of light (<0.1 mW/mm^2) and gradually increasing the light intensity until an EPSC was observed in an all-or-none manner. At the threshold intensity, trials that fail to evoke an EPSC were infrequently interleaved with successful trials. The ORN-PN synapse is highly reliable, with a single ORN spike evoking robust release of many synaptic vesicles at the ORN terminal[49]; thus, we interpret these failures as a failure to recruit a spike in a presynaptic axon on that trial (as opposed to a failure in synaptic transmission). As the light intensity was further increased, EPSC amplitude remained relatively constant, until it was observed to suddenly double, reflecting the recruitment of a second ORN axon. The mean

uEPSC for each PN was determined by averaging the evoked EPSC in ~8-12 trials at a light intensity approximately halfway between the initial threshold intensity and the doubling intensity. Recordings were discarded if any of the following criteria occurred: 1) a high rate of failures at the light intensity chosen for data collection (>10%); 2) uEPSC amplitude was not stable over a range of at least ~5 μW spanning the chosen light intensity; 2) the shape of the uEPSC was not stable.

Data Analysis

Unless otherwise stated, all analyses were performed in MATLAB (Mathworks, Natick, MA).

Quantification of electrophysiological responses

Analysis of neural responses was performed masked to the experimental condition (odor- versus solvent-exposed) of the recording. For each odor stimulus measurement in a fly, a trial block was comprised of 5 stimulus presentations for ORN responses, or 6 presentations for PN responses, at an intertrial interval of 40 s. The first trial for PN responses was not included in the analysis. Spike times were determined from raw ORN and PN voltage traces using custom scripts in MATLAB that identified spikes by thresholding on the first- and second-derivatives of the voltage. All spikes were manually inspected. Spike times were converted into a peristimulus time histogram (PSTH) by counting the number of spikes in 50-ms bins, overlapping by 25 ms. Single-trial PSTHs were averaged to generate a mean PSTH that describes the odor response for each cell. For membrane potential, single-trial voltage traces were averaged to generate a mean depolarization response for each cell. For each DL5 and VM7 PN, the response magnitude for each stimulus was computed as the trial-averaged spike rate (or membrane potential) during the 500-ms odor stimulus period, minus the trial-averaged spontaneous firing rate (or membrane potential) during the preceding 500 ms. For VA6 PNs, the response magnitude was computed over a 1000-ms window that begins at stimulus onset, which better captured the protracted odor

response (which extends into the post-stimulus period) observed in this cell type. A mean response magnitude was computed across trials for each experiment, and the overall mean response was plotted as mean ± SEM across all experiments in each condition.

Analysis of LN anatomical innervation

Images of all antennal lobes were collected with identical laser power and imaging settings (magnification, detector gain, offset, pixel size, and dwell time). Brains in which >0.01% of pixels in neuropil regions (excluding cell bodies and primary neurites) were high or low saturated were rejected. Confocal image stacks were imported into ImageJ (NIH) for analysis. Analysis of LN innervation was conducted masked to the experimental condition (odor- versus solvent-exposed). The boundaries of glomeruli of interest were manually traced in every third slice using the nc82 neuropil signal, guided by published atlases[17,100], and then interpolated through the stack to obtain the boundaries in adjacent slices. The 3D ROI manager plugin[101] was used to group together sets of ROIs across slices corresponding to each glomerulus to define the volumetric boundaries for each glomerulus and was then used for quantification of glomerular volume (number of pixels) and pixel intensities in each channel. For each 3D ROI corresponding to an individual identified glomerulus, LN neurites or neuropil per volume was computed as the sum of the pixel values in the ROI in the anti-CD8 (LN neurites) or nc82 (neuropil) channels, respectively, divided by the total number of pixels. The ratio of LN neurites to neuropil was computed as the sum of the pixel values in the ROI in the anti-CD8 channel divided by the sum of the pixel values in the ROI in the nc82 channel. To combine measurements across all glomeruli for a given metric (e.g. volume, LN neurites per volume, etc.), the measurement for each glomerulus in an experiment was normalized to the mean value for that glomerulus across all experiments in the solvent-exposed control condition. Plots show mean and standard error across brains.

Analysis of calcium imaging

The duration of each calcium imaging trial was 15 s, collected at 11 frames per second and 256x96 pixels per frame. Stimulus-evoked calcium signals (ΔF/F) were quantified from background-subtracted movies as the change in fluorescence ($F-F_0$) normalized to the mean fluorescence during the baseline period of each trial (F_0, averaged over 70 frames immediately preceding the odor), computed on a pixel-by-pixel basis in each frame. A Gaussian lowpass filter of size 4×4 pixels was applied to raw ΔF/F heatmaps.

A region-of-interest (ROI) was manually traced around each DL5 glomerulus, which contain the ab4a ORN terminals. ΔF/F signals were averaged across the pixels in the two DL5 ROIs and across three trials for each stimulus in an experiment. The odor response to the 500-ms stimulus presentation was typically captured in ~6 frames. The peak response for each experiment was quantified from the frame containing the maximum mean ΔF/F signal during the stimulus presentation. The overall mean response was plotted as mean ± SEM across all experiments in each condition.

Statistics

A permutation analysis was used to evaluate differences between experimental groups because of its conceptual simplicity and because it does not require assumptions about the underlying distribution of the population. For each measurement (e.g., the response of a PN type to an odor stimulus), experimental observations from flies in odor- and solvent-exposed conditions were combined and randomly reassigned into two groups (maintaining the number of samples in each respective experimental group), and the difference between the means of the groups was computed. This permutation process was repeated 10,000 times without replacement to generate a distribution for the difference between the means of the odor- and

990 solvent-exposed groups (see Figure 6 – figure supplement 1 for an example), under the null
991 assumption that there is no difference between the two populations. We calculated the fraction
992 of the empirically resampled distribution which had an absolute value that equaled or exceeded
993 the absolute observed difference between the means of the odor- and solvent-exposed groups
994 to determine the two-tailed p-value that the observed outcome occurred by chance if the
995 populations are not different. The cut-off for statistical significance of α=0.05 was adjusted to
996 account for multiple comparisons in an experiment using a Bonferroni correction. Permutation
997 testing was used in all figures, except in Figure 5 where the Mann-Whitney *U*-test was used,
998 implemented in MATLAB (Wilcoxon rank sum test).

999 Sample sizes were not predetermined using a power analysis. We used sample sizes
1000 comparable to those used in similar types of studies (e.g.,[6,8,99]). The experimenter was not
1001 masked to experimental condition or genotype during data collection. For a subset of analyses
1002 (analysis of electrophysiological data and quantification of LN innervation), the analyst was
1003 masked to the experimental condition, as described above.

1004

1005 DECLARATION OF INTERESTS

1006 The authors declare no competing interests.

1007

1008 DATA & MATERIALS AVAILABILITY STATEMENT

1009 The new transgenic fly generated in this study, *Or7a-lexA* (III), will be deposited in the
1010 Bloomington Drosophila Resource Center for public distribution. Source data from
1011 electrophysiology, functional imaging, and confocal imaging experiments used to
1012 generate Figures 2-7 are publicly available on the Dryad repository
1013 (https://doi.org/10.5061/dryad.v15dv420q).

ACKNOWLEDGEMENTS

We thank Chris Potter for the gift of Or7a-KI flies. We thank Meike Lobb-Rabe for generating the Or7a-lexA flies. We thank Daniel Wagenaar and the Caltech Neurotechnology Center for technical support in constructing fly holders and custom odor delivery devices. We thank members of the Hong laboratory for their critical reading and feedback on this manuscript. This work was supported by grants from the National Science Foundation (Award #1556230), the Shurl and Kay Curci Foundation, and the National Institutes of Health (1RF1MH117825). E.J.H. was supported by a Clare Boothe Luce professorship.

REFERENCES

1. Espinosa, J.S., and Stryker, M.P. (2012). Development and Plasticity of the Primary Visual Cortex. Neuron *75*, 230–249. 10.1016/j.neuron.2012.06.009.

2. Barlow, H.G. (1961). Possible principles underlying the transformation of sensory messages. In Sensory Communication, W. A. Rosenblith, ed. (MIT Press), pp. 217–234.

3. Fiser, J., Berkes, P., Orban, G., and Lengyel, M. (2010). Statistically optimal perception and learning: from behavior to neural representations. Trends in cognitive sciences *14*, 119–130. 10.1016/j.tics.2010.01.003.

4. Gilbert, C.D., Li, W., and Piech, V. (2009). Perceptual learning and adult cortical plasticity. The Journal of physiology *587*, 2743–2751. 10.1113/jphysiol.2009.171488.

5. Pienkowski, M., and Eggermont, J.J. (2011). Cortical tonotopic map plasticity and behavior. Neurosci Biobehav Rev *35*, 2117–2128. 10.1016/j.neubiorev.2011.02.002.

6. Das, S., Sadanandappa, M.K., Dervan, A., Larkin, A., Lee, J.A., Sudhakaran, I.P., Priya, R., Heidari, R., Holohan, E.E., Pimentel, A., et al. (2011). Plasticity of local GABAergic interneurons drives olfactory habituation. Proc Natl Acad Sci U S A *108*, E646–E654. 10.1073/pnas.1106411108.

7. Kreile, A.K., Bonhoeffer, T., and Hübener, M. (2011). Altered Visual Experience Induces Instructive Changes of Orientation Preference in Mouse Visual Cortex. J Neurosci *31*, 13911–13920. 10.1523/JNEUROSCI.2143-11.2011.

1044 8. Sachse, S., Rueckert, E., Keller, A., Okada, R., Tanaka, N.K., Ito, K., and Vosshall, L.B.
1045 (2007). Activity-dependent plasticity in an olfactory circuit. Neuron *56*, 838–850.
1046 10.1016/j.neuron.2007.10.035.

1047 9. Sengpiel, F., Stawinski, P., and Bonhoeffer, T. (1999). Influence of experience on
1048 orientation maps in cat visual cortex. Nat Neurosci *2*, 727–732. 10.1038/11192.

1049 10. Wilson, D.A., Sullivan, R.M., and Leon, M. (1985). Odor Familiarity Alters Mitral Cell
1050 Response in the Olfactory Bulb of Neonatal Rats. Developmental Brain Research *22*, 314–317.
1051 10.1016/0165-3806(85)90186-5.

1052 11. Zhang, L.I., Bao, S., and Merzenich, M.M. (2001). Persistent and specific influences of
1053 early acoustic environments on primary auditory cortex. Nat Neurosci *4*, 1123–1130.
1054 10.1038/nn745.

1055 12. Ressler, K.J., Sullivan, S.L., and Buck, L.B. (1994). Information coding in the olfactory
1056 system: evidence for a stereotyped and highly organized epitope map in the olfactory bulb.
1057 Cell *79*, 1245–1255.

1058 13. Vassar, R., Chao, S.K., Sitcheran, R., Nunez, J.M., Vosshall, L.B., and Axel, R. (1994).
1059 Topographic organization of sensory projections to the olfactory bulb. Cell *79*, 981–991.

1060 14. Vosshall, L.B., and Stocker, R.F. (2007). Molecular architecture of smell and taste in
1061 Drosophila. Annu Rev Neurosci *30*, 505–533. 10.1146/annurev.neuro.30.051606.094306.

1062 15. Vosshall, L.B., Wong, A.M., and Axel, R. (2000). An olfactory sensory map in the fly
1063 brain. Cell *102*, 147–159.

1064 16. Stocker, R.F., Lienhard, M.C., Borst, A., and Fischbach, K.F. (1990). Neuronal
1065 architecture of the antennal lobe in Drosophila melanogaster. Cell and Tissue Research *262*, 9–
1066 34.

1067 17. Couto, A., Alenius, M., and Dickson, B.J. (2005). Molecular, anatomical, and functional
1068 organization of the Drosophila olfactory system. Current Biology *15*, 1535–1547.

1069 18. Fishilevich, E., and Vosshall, L.B. (2005). Genetic and functional subdivision of the
1070 Drosophila antennal lobe. Current Biology *15*, 1548–1553.

1071 19. Silbering, A.F., Rytz, R., Grosjean, Y., Abuin, L., Ramdya, P., Jefferis, G.S., and Benton,
1072 R. (2011). Complementary function and integrated wiring of the evolutionarily distinct
1073 Drosophila olfactory subsystems. The Journal of neuroscience : the official journal of the
1074 Society for Neuroscience *31*, 13357–13375. 10.1523/JNEUROSCI.2360-11.2011.

1075 20. de Bruyne, M., Clyne, P.J., and Carlson, J.R. (1999). Odor coding in a model olfactory
1076 organ: the Drosophila maxillary palp. J. Neurosci. *19*, 4520–4532.

1077 21. de Bruyne, M., Foster, K., and Carlson, J.R. (2001). Odor coding in the Drosophila
1078 antenna. Neuron *30*, 537–552.

22. Hallem, E.A., and Carlson, J.R. (2006). Coding of odors by a receptor repertoire. Cell *125*, 143–160.

23. Hallem, E.A., Ho, M.G., and Carlson, J.R. (2004). The molecular basis of odor coding in the Drosophila antenna. Cell *117*, 965–979.

24. Olsen, S.R., Bhandawat, V., and Wilson, R.I. (2010). Divisive normalization in olfactory population codes. Neuron *66*, 287–299. 10.1016/j.neuron.2010.04.009.

25. Schlief, M.L., and Wilson, R.I. (2007). Olfactory processing and behavior downstream from highly selective receptor neurons. Nature Neuroscience *10*, 623–630.

26. Mandairon, N., and Linster, C. (2009). Odor Perception and Olfactory Bulb Plasticity in Adult Mammals. Journal of Neurophysiology *101*, 2204–2209. 10.1152/jn.00076.2009.

27. Mandairon, N., Stack, C., Kiselycznyk, C., and Linster, C. (2006). Enrichment to odors improves olfactory discrimination in adult rats. Behav Neurosci *120*, 173–179. 10.1037/0735-7044.120.1.173.

28. Liu, A., and Urban, N.N. (2017). Prenatal and Early Postnatal Odorant Exposure Heightens Odor-Evoked Mitral Cell Responses in the Mouse Olfactory Bulb. eNeuro *4*. 10.1523/ENEURO.0129-17.2017.

29. Liu, A., Savya, S., and Urban, N.N. (2016). Early Odorant Exposure Increases the Number of Mitral and Tufted Cells Associated with a Single Glomerulus. J. Neurosci. *36*, 11646–11653. 10.1523/JNEUROSCI.0654-16.2016.

30. Todrank, J., Heth, G., and Restrepo, D. (2011). Effects of in utero odorant exposure on neuroanatomical development of the olfactory bulb and odour preferences. Proc Biol Sci *278*, 1949–1955. 10.1098/rspb.2010.2314.

31. Woo, C.C., Hingco, E.E., Taylor, G.E., and Leon, M. (2006). Exposure to a broad range of odorants decreases cell mortality in the olfactory bulb. Neuroreport *17*, 817–821. 10.1097/01.wnr.0000215780.84226.2d.

32. Golovin, R.M., and Broadie, K. (2016). Developmental experience-dependent plasticity in the first synapse of the Drosophila olfactory circuit. J Neurophysiol *116*, 2730–2738. 10.1152/jn.00616.2016.

33. Twick, I., Lee, J.A., and Ramaswami, M. (2014). Chapter 1 - Olfactory Habituation in Drosophila—Odor Encoding and its Plasticity in the Antennal Lobe. In Progress in Brain Research Odor Memory and Perception., E. Barkai and D. A. Wilson, eds. (Elsevier), pp. 3–38. 10.1016/B978-0-444-63350-7.00001-2.

34. Bai, Y., and Suzuki, T. (2020). Activity-Dependent Synaptic Plasticity in Drosophila melanogaster. Frontiers in Physiology *11*.

35. Devaud, J.M., Acebes, A., and Ferrus, A. (2001). Odor exposure causes central adaptation and morphological changes in selected olfactory glomeruli in Drosophila. The Journal of neuroscience : the official journal of the Society for Neuroscience *21*, 6274–6282.

36. Devaud, J.M., Acebes, A., Ramaswami, M., and Ferrus, A. (2003). Structural and functional changes in the olfactory pathway of adult Drosophila take place at a critical age. Journal of neurobiology *56*, 13–23. 10.1002/neu.10215.

37. Golovin, R.M., Vest, J., Vita, D.J., and Broadie, K. (2019). Activity-Dependent Remodeling of Drosophila Olfactory Sensory Neuron Brain Innervation during an Early-Life Critical Period. J. Neurosci. *39*, 2995–3012. 10.1523/JNEUROSCI.2223-18.2019.

38. Kidd, S., Struhl, G., and Lieber, T. (2015). Notch is required in adult Drosophila sensory neurons for morphological and functional plasticity of the olfactory circuit. PLoS genetics *11*, e1005244. 10.1371/journal.pgen.1005244.

39. Chodankar, A., Sadanandappa, M.K., VijayRaghavan, K., and Ramaswami, M. (2020). Glomerulus-Selective Regulation of a Critical Period for Interneuron Plasticity in the Drosophila Antennal Lobe. J. Neurosci. *40*, 5549–5560. 10.1523/JNEUROSCI.2192-19.2020.

40. Sudhakaran, I.P., Holohan, E.E., Osman, S., Rodrigues, V., VijayRaghavan, K., and Ramaswami, M. (2012). Plasticity of Recurrent Inhibition in the Drosophila Antennal Lobe. J. Neurosci. *32*, 7225–7231. 10.1523/JNEUROSCI.1099-12.2012.

41. Hong, E.J., and Wilson, R.I. (2015). Simultaneous encoding of odors by channels with diverse sensitivity to inhibition. Neuron *85*, 573–589. 10.1016/j.neuron.2014.12.040.

42. Wilson, R.I. (2013). Early olfactory processing in Drosophila: mechanisms and principles. Annual Review of Neuroscience *36*, in press.

43. Nagel, K.I., and Wilson, R.I. (2011). Biophysical mechanisms underlying olfactory receptor neuron dynamics. Nature neuroscience *14*, 208–216. 10.1038/nn.2725.

44. Olsen, S.R., and Wilson, R.I. (2008). Lateral presynaptic inhibition mediates gain control in an olfactory circuit. Nature *452*, 956–960.

45. Chakraborty, T.S., Goswami, S.P., and Siddiqi, O. (2009). Sensory Correlates of Imaginal Conditioning in Drosophila melanogaster. Journal of Neurogenetics *23*, 210–219. 10.1080/01677060802491559.

46. Iyengar, A., Chakraborty, T.S., Goswami, S.P., Wu, C.-F., and Siddiqi, O. (2010). Post-eclosion odor experience modifies olfactory receptor neuron coding in Drosophila. PNAS *107*, 9855–9860. 10.1073/pnas.1003856107.

47. Grabe, V., Baschwitz, A., Dweck, H.K.M., Lavista-Llanos, S., Hansson, B.S., and Sachse, S. (2016). Elucidating the Neuronal Architecture of Olfactory Glomeruli in the Drosophila Antennal Lobe. Cell Reports *16*, 3401–3413. 10.1016/j.celrep.2016.08.063.

48. Horne, J.A., Langille, C., McLin, S., Wiederman, M., Lu, Z., Xu, C.S., Plaza, S.M., Scheffer, L.K., Hess, H.F., and Meinertzhagen, I.A. (2018). A resource for the Drosophila antennal lobe provided by the connectome of glomerulus VA1v. eLife *7*, e37550. 10.7554/eLife.37550.

1152 49. Kazama, H., and Wilson, R.I. (2008). Homeostatic matching and nonlinear amplification
1153 at genetically-identified central synapses. Neuron *58*, 401–413.

1154 50. Rybak, J., Talarico, G., Ruiz, S., Arnold, C., Cantera, R., and Hansson, B.S. (2016).
1155 Synaptic circuitry of identified neurons in the antennal lobe of Drosophila melanogaster.
1156 Journal of Comparative Neurology *524*, 1920–1956. 10.1002/cne.23966.

1157 51. Tobin, W.F., Wilson, R.I., and Lee, W.-C.A. (2017). Wiring variations that enable and
1158 constrain neural computation in a sensory microcircuit. eLife *6*, e24838. 10.7554/eLife.24838.

1159 52. Klapoetke, N.C., Murata, Y., Kim, S.S., Pulver, S.R., Birdsey-Benson, A., Cho, Y.K.,
1160 Morimoto, T.K., Chuong, A.S., Carpenter, E.J., Tian, Z., et al. (2014). Independent optical
1161 excitation of distinct neural populations. Nature methods *11*, 338–346. 10.1038/nmeth.2836.

1162 53. Jeanne, J.M., and Wilson, R.I. (2015). Convergence, Divergence, and Reconvergence in
1163 a Feedforward Network Improves Neural Speed and Accuracy. Neuron *88*, 1014–1026.
1164 10.1016/j.neuron.2015.10.018.

1165 54. Olsen, S.R., Bhandawat, V., and Wilson, R.I. (2007). Excitatory interactions between
1166 olfactory processing channels in the Drosophila antennal lobe. Neuron *54*, 89–103.

1167 55. Root, C.M., Semmelhack, J.L., Wong, A.M., Flores, J., and Wang, J.W. (2007).
1168 Propagation of olfactory information in Drosophila. Proceedings of the National Academy of
1169 Sciences of the United States of America *104*, 11826–11831.

1170 56. Shang, Y., Claridge-Chang, A., Sjulson, L., Pypaert, M., and Miesenbock, G. (2007).
1171 Excitatory local circuits and their implications for olfactory processing in the fly antennal lobe.
1172 Cell *128*, 601–612.

1173 57. Yaksi, E., and Wilson, R.I. (2010). Electrical coupling between olfactory glomeruli.
1174 Neuron *67*, 1034–1047. 10.1016/j.neuron.2010.08.041.

1175 58. Wang, H.W., Wysocki, C.J., and Gold, G.H. (1993). Induction of olfactory receptor
1176 sensitivity in mice. Science *260*, 998–1000. 10.1126/science.8493539.

1177 59. Boschetti, A., Biasioli, F., van Opbergen, M., Warneke, C., Jordan, A., Holzinger, R.,
1178 Prazeller, P., Karl, T., Hansel, A., Lindinger, W., et al. (1999). PTR-MS real time monitoring of
1179 the emission of volatile organic compounds during postharvest aging of berryfruit. Postharvest
1180 Biology and Technology *17*, 143–151. 10.1016/S0925-5214(99)00052-6.

1181 60. Farneti, B., Khomenko, I., Grisenti, M., Ajelli, M., Betta, E., Algarra, A.A., Cappellin, L.,
1182 Aprea, E., Gasperi, F., Biasioli, F., et al. (2017). Exploring Blueberry Aroma Complexity by
1183 Chromatographic and Direct-Injection Spectrometric Techniques. Front. Plant Sci. *8*.
1184 10.3389/fpls.2017.00617.

1185 61. Jordán, M.J., Tandon, K., Shaw, P.E., and Goodner, K.L. (2001). Aromatic Profile of
1186 Aqueous Banana Essence and Banana Fruit by Gas Chromatography−Mass Spectrometry
1187 (GC-MS) and Gas Chromatography−Olfactometry (GC-O). J. Agric. Food Chem. *49*, 4813–
1188 4817. 10.1021/jf010471k.

62. CDC - Immediately Dangerous to Life or Health Concentrations (IDLH) (2019). https://www.cdc.gov/niosh/idlh/default.html.

63. Steinemann, A. (2016). Fragranced consumer products: exposures and effects from emissions. Air Qual Atmos Health *9*, 861–866. 10.1007/s11869-016-0442-z.

64. Wolkoff, P., and Nielsen, G.D. (2017). Effects by inhalation of abundant fragrances in indoor air – An overview. Environment International *101*, 96–107. 10.1016/j.envint.2017.01.013.

65. Wypych, G. (2017). Handbook of Odors in Plastic Materials (Elsevier).

66. Mandairon, N., Stack, C., Kiselycznyk, C., and Linster, C. (2006). Broad activation of the olfactory bulb produces long-lasting changes in odor perception. PNAS *103*, 13543–13548. 10.1073/pnas.0602750103.

67. Rochefort, C., Gheusi, G., Vincent, J.-D., and Lledo, P.-M. (2002). Enriched Odor Exposure Increases the Number of Newborn Neurons in the Adult Olfactory Bulb and Improves Odor Memory. J. Neurosci. *22*, 2679–2689. 10.1523/JNEUROSCI.22-07-02679.2002.

68. Beaulieu, C., and Cynader, M. (1990). Effect of the richness of the environment on neurons in cat visual cortex. I. Receptive field properties. Brain Res. Dev. Brain Res. *53*, 71–81. 10.1016/0165-3806(90)90125-i.

69. Beaulieu, C., and Cynader, M. (1990). Effect of the richness of the environment on neurons in cat visual cortex. II. Spatial and temporal frequency characteristics. Brain Res. Dev. Brain Res. *53*, 82–88. 10.1016/0165-3806(90)90126-j.

70. Engineer, N.D., Percaccio, C.R., Pandya, P.K., Moucha, R., Rathbun, D.L., and Kilgard, M.P. (2004). Environmental Enrichment Improves Response Strength, Threshold, Selectivity, and Latency of Auditory Cortex Neurons. Journal of Neurophysiology *92*, 73–82. 10.1152/jn.00059.2004.

71. Stopfer, M., and Laurent, G. (1999). Short-term memory in olfactory network dynamics. Nature *402*, 664–668. 10.1038/45244.

72. Franco, L.M., and Yaksi, E. (2021). Experience-dependent plasticity modulates ongoing activity in the antennal lobe and enhances odor representations. Cell Reports *37*, 110165. 10.1016/j.celrep.2021.110165.

73. Bazhenov, M., Stopfer, M., Sejnowski, T.J., and Laurent, G. (2005). Fast odor learning improves reliability of odor responses in the locust antennal lobe. Neuron *46*, 483–492.

74. Cadiou, H., Aoudé, I., Tazir, B., Molinas, A., Fenech, C., Meunier, N., and Grosmaitre, X. (2014). Postnatal Odorant Exposure Induces Peripheral Olfactory Plasticity at the Cellular Level. J. Neurosci. *34*, 4857–4870. 10.1523/JNEUROSCI.0688-13.2014.

75. Cavallin, M.A., Powell, K., Biju, K.C., and Fadool, D.A. (2010). State-dependent sculpting of olfactory sensory neurons is attributed to sensory enrichment, odor deprivation, and aging. Neurosci. Lett. *483*, 90–95. 10.1016/j.neulet.2010.07.059.

76. Kass, M.D., Moberly, A.H., Rosenthal, M.C., Guang, S.A., and McGann, J.P. (2013). Odor-Specific, Olfactory Marker Protein-Mediated Sparsening of Primary Olfactory Input to the Brain after Odor Exposure. J. Neurosci. *33*, 6594–6602. 10.1523/JNEUROSCI.1442-12.2013.

77. Santoro, S.W., and Dulac, C. (2012). The activity-dependent histone variant H2BE modulates the life span of olfactory neurons. Elife *1*, e00070. 10.7554/eLife.00070.

78. Watt, W.C., Sakano, H., Lee, Z.-Y., Reusch, J.E., Trinh, K., and Storm, D.R. (2004). Odorant stimulation enhances survival of olfactory sensory neurons via MAPK and CREB. Neuron *41*, 955–967. 10.1016/s0896-6273(04)00075-3.

79. Kazama, H., Yaksi, E., and Wilson, R.I. (2011). Cell death triggers olfactory circuit plasticity via glial signaling in Drosophila. The Journal of neuroscience : the official journal of the Society for Neuroscience *31*, 7619–7630. 10.1523/JNEUROSCI.5984-10.2011.

80. Dylla, K.V., O'Connell, T.F., and Hong, E.J. Early life experience with natural odors modifies olfactory behavior through an associative process.

81. Heisenberg, M. (2003). Mushroom body memoir: from maps to models. Nature reviews. Neuroscience *4*, 266–275. 10.1038/nrn1074.

82. Cang, J., and Feldheim, D.A. (2013). Developmental Mechanisms of Topographic Map Formation and Alignment. Annual Review of Neuroscience *36*, 51–77. 10.1146/annurev-neuro-062012-170341.

83. Huberman, A.D., Feller, M.B., and Chapman, B. (2008). Mechanisms Underlying Development of Visual Maps and Receptive Fields. Annual Review of Neuroscience *31*, 479–509. 10.1146/annurev.neuro.31.060407.125533.

84. D'Orazi, F.D., Suzuki, S.C., and Wong, R.O. (2014). Neuronal remodeling in retinal circuit assembly, disassembly, and reassembly. Trends in Neurosciences *37*, 594–603. 10.1016/j.tins.2014.07.009.

85. Elstrott, J., and Feller, M.B. (2009). Vision and the establishment of direction-selectivity: a tale of two circuits. Current Opinion in Neurobiology *19*, 293–297. 10.1016/j.conb.2009.03.004.

86. Li, Y., Fitzpatrick, D., and White, L.E. (2006). The development of direction selectivity in ferret visual cortex requires early visual experience. Nat Neurosci *9*, 676–681. 10.1038/nn1684.

87. Li, Y., Hooser, S.D.V., Mazurek, M., White, L.E., and Fitzpatrick, D. (2008). Experience with moving visual stimuli drives the early development of cortical direction selectivity. Nature *456*, 952–956. 10.1038/nature07417.

88. Chan, Y.-C., and Chiao, C.-C. (2008). Effect of visual experience on the maturation of ON–OFF direction selective ganglion cells in the rabbit retina. Vision Research *48*, 2466–2475. 10.1016/j.visres.2008.08.010.

89. Elstrott, J., Anishchenko, A., Greschner, M., Sher, A., Litke, A.M., Chichilnisky, E.J., and Feller, M.B. (2008). Direction Selectivity in the Retina Is Established Independent of Visual

1262 Experience and Cholinergic Retinal Waves. Neuron *58*, 499–506.
1263 10.1016/j.neuron.2008.03.013.

1264 90. Hayashi, S., Ito, K., Sado, Y., Taniguchi, M., Akimoto, A., Takeuchi, H., Aigaki, T.,
1265 Matsuzaki, F., Nakagoshi, H., Tanimura, T., et al. (2002). GETDB, a database compiling
1266 expression patterns and molecular locations of a collection of gal4 enhancer traps. genesis *34*,
1267 58–61. 10.1002/gene.10137.

1268 91. Marin, E.C., Watts, R.J., Tanaka, N.K., Ito, K., and Luo, L. (2005). Developmentally
1269 programmed remodeling of the Drosophila olfactory circuit. Development *132*, 725–737.

1270 92. Lin, C.-C., Prokop-Prigge, K.A., Preti, G., and Potter, C.J. (2015). Food odors trigger
1271 Drosophila males to deposit a pheromone that guides aggregation and female oviposition
1272 decisions. eLife *4*, e08688. 10.7554/eLife.08688.

1273 93. Lee, T., and Luo, L. (1999). Mosaic analysis with a repressible cell marker for studies of
1274 gene function in neuronal morphogenesis. Neuron *22*, 451–461.

1275 94. Pfeiffer, B.D., Ngo, T.T., Hibbard, K.L., Murphy, C., Jenett, A., Truman, J.W., and Rubin,
1276 G.M. (2010). Refinement of tools for targeted gene expression in Drosophila. Genetics *186*,
1277 735–755. 10.1534/genetics.110.119917.

1278 95. Fouquet, W., Owald, D., Wichmann, C., Mertel, S., Depner, H., Dyba, M., Hallermann,
1279 S., Kittel, R.J., Eimer, S., and Sigrist, S.J. (2009). Maturation of active zone assembly by
1280 Drosophila Bruchpilot. Journal of Cell Biology *186*, 129–145. 10.1083/jcb.200812150.

1281 96. Chen, T.W., Wardill, T.J., Sun, Y., Pulver, S.R., Renninger, S.L., Baohan, A., Schreiter,
1282 E.R., Kerr, R.A., Orger, M.B., Jayaraman, V., et al. (2013). Ultrasensitive fluorescent proteins for
1283 imaging neuronal activity. Nature *499*, 295–300. 10.1038/nature12354.

1284 97. Kim, S., Chen, J., Cheng, T., Gindulyte, A., He, J., He, S., Li, Q., Shoemaker, B.A.,
1285 Thiessen, P.A., Yu, B., et al. (2021). PubChem in 2021: new data content and improved web
1286 interfaces. Nucleic Acids Research *49*, D1388–D1395. 10.1093/nar/gkaa971.

1287 98. Wilson, R.I., Turner, G.C., and Laurent, G. (2004). Transformation of olfactory
1288 representations in the Drosophila antennal lobe. Science *303*, 366–370.

1289 99. Bhandawat, V., Olsen, S.R., Schlief, M.L., Gouwens, N.W., and Wilson, R.I. (2007).
1290 Sensory processing in the Drosophila antennal lobe increases the reliability and separability of
1291 ensemble odor representations. Nature Neuroscience *10*, 1474–1482.

1292 100. Laissue, P.P., Reiter, C., Hiesinger, P.R., Halter, S., Fischbach, K.F., and Stocker, R.F.
1293 (1999). Three-dimensional reconstruction of the antennal lobe in Drosophila melanogaster.
1294 Journal of Comparative Neurology *405*, 543–552.

1295 101. Ollion, J., Cochennec, J., Loll, F., Escudé, C., and Boudier, T. (2013). TANGO: a generic
1296 tool for high-throughput 3D image analysis for studying nuclear organization. Bioinformatics
1297 *29*, 1840–1841. 10.1093/bioinformatics/btt276.

1298